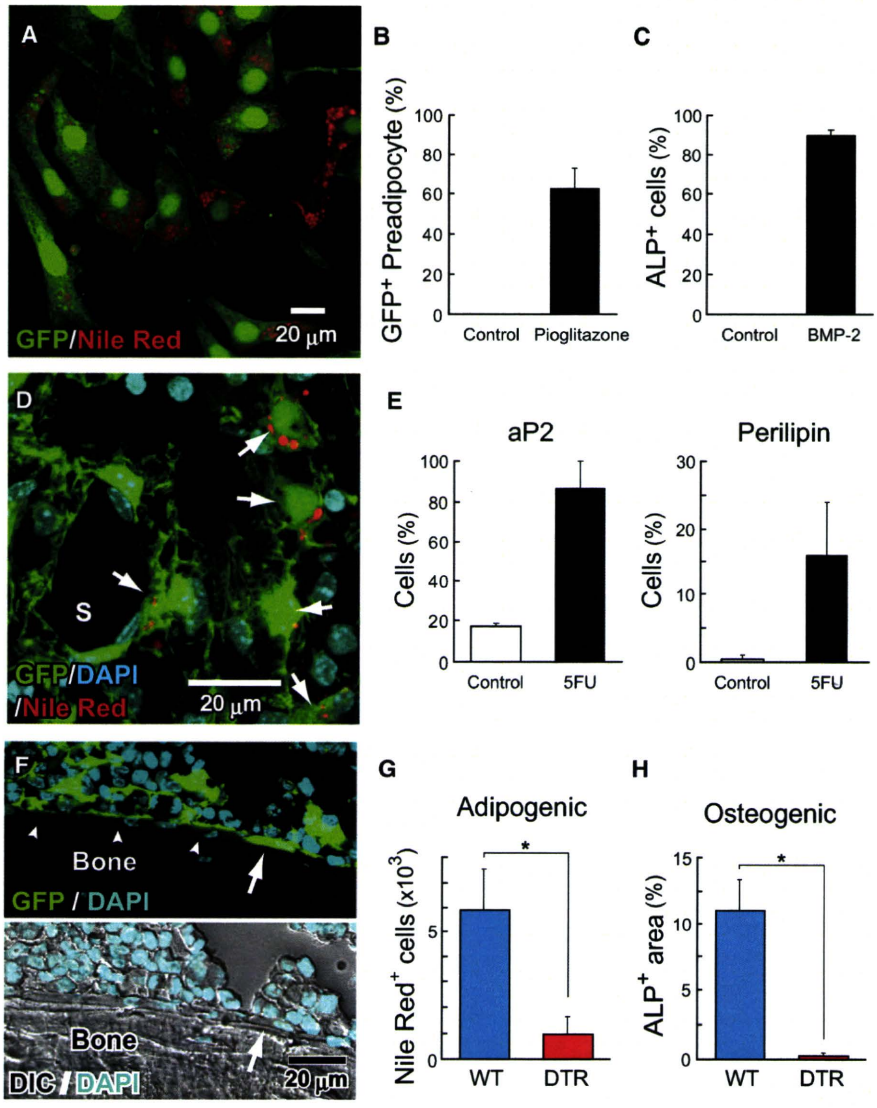

Figure 7. CAR Cells Have the Potential to Differentiate into Adipocytic and Osteoblastic Cells

(A-C) Bone marrow cells from CXCL12-GFP mice were cultured with pioglitazone (A and B) or BMP-2 (C). (A and B) After 7 days, cultures were analyzed by Nile Red staining. (A) Lipid inclusions (red) within the cytoplasm of CAR cells (green). (B) Frequency of lipid-containing cells in the whole CAR cells. (C) After 4 days, ALP activity was assayed by Fast Red staining. Frequency of ALP activity-containing cells in whole CAR cells.

(D and E) CXCL12-GFP mice were analyzed 7 days after administration of 5-FU or control vehicle. (D) Bone marrow sections stained with Nile Red. Lipid inclusions (arrows; red) within the cytoplasm of some CAR cells (green). (E) Single-cell RT-PCR analysis of the frequency of cells expressing aP2 (left) and perilipin (right) in sorted CAR cells.

(F) The bone marrow sections from 3-week-old growing CXCL12-GFP mice. Some CAR cells (green) are in contact with (arrowheads) or inserted into (arrow) the layer of mature osteoblasts lining the bone surface.

(G and H) Whole bone marrow cells from wild-type and CXCL12-DTR-GFP mice at 2 days after DT administration were cultured with pioglitazone (G) or BMP-2 (H). (G) After 7 days, cultures were analyzed by Nile Red staining. Numbers of lipid-containing cells are shown. (H) After 4 days, ALP activity was assayed by Fast Red staining. The percentage of the ALP-positive area relative to the culture area is shown. All error bars represent SD of the mean; n = 4; *p < 0.05 (B, C, E, G and H). The nuclei of cells were labeled with DAPI dye (blue) (D and F).

not (Figure 7D). Additionally, single-cell RT-PCR analysis revealed that the frequencies of cells expressing aP2, an adipocyte-specific fatty acid binding protein, and perilipin, a protein coating lipid droplets of adipocytes, which is essential for adipogenesis (Martinez-Botas et al., 2000) within CAR cells, were elevated from 17% and 0.49% in untreated mice to 87% and 16% in mice 7 days after 5-FU injection, respectively (Figure 7E), suggesting that some CAR cells differentiated into adipocytes in vivo after 5-FU-induced bone marrow hypoplasia.

In addition, immunohistochemical analysis of 3-week-old growing CXCL12-GFP mice has shown that some CAR cells are in contact with or inserted into the layer of CXCL12-GFP$^-$ mature osteoblasts lining the bone surface, raising the possibility that CAR cells near the bone surface differentiate into mature osteoblasts in vivo (Figure 7F). Together, these results suggest that the majority of CAR cells have the potential to differentiate into adipocytic and osteoblastic cells, and the differentiation of some CAR cells occurs in vivo.

Finally, we analyzed the ability of CAR cell-depleted bone marrow cells to differentiate into adipocytic and osteoblastic cells. We cultured whole bone marrow cells from DT-treated CXCL12-DTR-GFP mice and control animals in medium containing pioglitazone or BMP-2. The numbers of lipid-containing adipocytic cells or marked ALP activity-containing osteoblastic cells were severely reduced in cultures from CAR cell-depleted bone marrow cells compared with cultures from control bone marrow cells, as assessed by Nile Red or Fast Red staining, respectively (Figures 7G and 7H and data not shown). These results support the idea that CAR cells are progenitors of adipocytes and osteoblasts within bone marrow.

DISCUSSION

In this study, we determined the in vivo essential role of CAR cells as the niche for HSCs and lymphoid and erythroid progenitors, using DT-treated CXCL12-DTR-GFP mice in which CAR cells were selectively lost but other candidate niches, including bone-lining osteoblasts, SNO cells, and endothelial cells, were still present. Together with the significant mRNA expression of Col1α1 in CAR cells, there is a possibility that CAR cells were decreased in the Col2.3ΔTK mice depleted of cells with the rat Col1α1 gene promoter driving thymidine kinase, in which B cells and erythrocytes were reduced (Visnjic et al., 2004). In addition,

because CAR cells exhibited high expression of BMPRIA and PPR, which have been reported to control HSC numbers, BMPRIA and/or PPR might regulate niche functions of CAR cells.

HSCs remained viable much longer than lymphoid and erythroid progenitors during cultures in serum alone and display similar phenotypes to HSCs from CAR cell-depleted mice. Considering that serum contains widely diffusible signals present in the circulation and marrow non-niche microenvironment, these results suggest that CAR cells are the major producer of specific niche signals for HSCs and hematopoietic progenitors in bone marrow. Because our results indicate that CAR cells are the major producer of SCF and CXCL12, which are essential for the maintenance of HSCs and lymphoid and erythroid progenitors, SCF and CXCL12 would contribute in concert with other factors to the niche functions of CAR cells.

Recent studies using label-retaining assays have identified a highly dormant small subpopulation (~30%) of HSCs, termed dormant HSCs (d-HSCs), dividing about every 145 days, and another rarely dividing activated HSC (a-HSCs) subpopulation (~70%) dividing around every 36 days, within the $CD34^{-}Lin^{-}$ $Sca\text{-}1^{+}c\text{-}kit^{+}CD150^{+}CD48^{-}$ HSC population of bone marrow (Wilson et al., 2008). Considering that HSCs were reduced and more quiescent in the absence of CAR cells, this raises the possibility that a-HSCs were selectively lost or returned to a d-HSC status in CAR cell-depleted mice. Further studies will be needed to determine the role of CAR cells in the maintenance of d-HSCs and a-HSCs.

Our findings suggest that CAR cells maintain both HSCs and B cell and erythroid progenitors in a proliferative state; however, HSCs are cycling slowly, although B cell and erythroid progenitors are cycling much more rapidly. How can we explain the difference? Infrequent division of HSCs may be controlled by HSC-intrinsic mechanisms. An alternative explanation is that CAR cells or other microenvironmental components located near CAR cells, including endothelial cells, provide signals that slow the proliferation of HSCs, but not lymphoid or erythroid progenitors. Candidates include Angiopoietin-1, Wnts, and TGF-βs, which have been reported to slow the proliferation of HSCs (Arai et al., 2004; Fleming et al., 2008; Yamazaki et al., 2009). In contrast, critical lineage-specific soluble factors, including IL-7 and erythropoietin, augment the proliferation of lymphoid and erythroid progenitors, respectively, but not HSCs.

Although niche signals maintain stem cells in an undifferentiated state in *Drosophila* gonads (Xie and Spradling, 1998), it remains unclear whether vertebrate HSC niches employ an analogous mechanism. Our findings that HSCs from CAR cell-depleted mice have a markedly increased mRNA expression of PU.1 and generate substantial numbers of myeloid lineage cells in culture earlier than the wild-type suggest that CAR cells keep HSCs in an undifferentiated state. It may be that myeloid differentiation of HSCs is a default pathway in the absence of niche signals that maintain HSCs in a proliferative state. Alternatively, CAR cells may provide signals which inhibit the myeloid differentiation of HSCs controlled by non-CAR cell microenvironmental factors and/or HSC-intrinsic mechanisms.

At 2 days after the induction of CAR cell ablation, the numbers of HSCs were reduced about 50% in the marrow. Because it has been reported that only about 4% of HSCs are proliferating at any given time (Kiel et al., 2005) and that HSCs divide every 36 or 145 days (Wilson et al., 2008), HSC reduction over 2 days in CAR cell-depleted mice cannot be explained simply by the results that CAR cells maintain HSCs in a proliferative state. It is likely that enhanced differentiation of some HSCs caused HSC reduction in CAR cell-depleted mice. In addition, although no increase in Annexin-V-positive apoptotic cells in the HSC fraction and the accumulation of HSCs in the circulation was observed in CAR cell-depleted mice, there is a possibility that CAR cells are also involved in supporting the survival and/or retention of HSCs within bone marrow.

CXCL12-DTR-GFP mice died probably from liver failure 5 days after DT treatment and it should also be noted that thrombopoietin (TPO), which plays a critical role in hematopoiesis is predominantly expressed in liver (Lok et al., 1994). However, at 2 days after DT treatment, the liver of CXCL12-DTR-GFP mice in which bone marrow hematopoiesis was affected appeared normal macroscopically and histologically, and had normal expression of TPO mRNA by qRT-PCR analysis (data not shown). In addition, there was no reduction of TPO protein in peripheral blood of the DT-treated CXCL12-DTR-GFP mice (data not shown). These results suggest that the liver of CXCL12-DTR-GFP mice did not cause the hematopoietic abnormalities 2 days after DT treatment. On the other hand, in the bone marrow of DT-treated CXCL12-DTR-GFP mice in which the numbers of CAR cells were reduced, the size of HSCs in contact with the remaining CAR cells was normal, although the size of HSCs which did not adjoin CAR cells was significantly reduced by histological analysis. Together, it is likely that phenotypes observed in the marrow of CXCL12-DTR-GFP mice were because of loss of CAR cells 2 days after DT treatment.

Our results do not rule out the possibility that other candidate niches, including SNO cells and endothelial cells, play an important role in hematopoiesis. The results that the numbers of MPPs, $CCR9^{+}$MPPs, and $CD122^{+}NK1.1^{-}$ NK progenitors were normal, although CLPs and $CCR9^{+}$CLPs (Zlotoff et al., 2010) were reduced in DT-treated CXCL12-DTR-GFP mice (Figure S2C), suggest that progenitors for distinct lymphoid lineages may inhabit different niches and have different requirements in bone marrow. Because many CAR cells are perivascular, interaction between CAR cells and endothelial cells may be important in the construction of HSC niches. Experiments using mice that allow the selective depletion of SNO cells or sinusoidal endothelial cells will be needed to determine the niche functions of these cells.

We have suggested that CAR cells are adipo-osteogenic progenitors, which produce large amounts of hematopoietic cytokines, CXCL12 and SCF, before they differentiate into mature cells producing large amounts of proteins for the storage of nutritional energy or bone formation. Previous studies have shown that adventitial reticular cells covering the endothelium of vascular sinuses give rise to adipocytes (Bianco et al., 1988) and that osteogenic progenitors are present in the intertrabecular space of bone marrow (Rouleau et al., 1990). Our results explain this discrepancy and suggest an essential in vivo role of adipo-osteogenic progenitors in bone marrow. In addition, our findings raise the possibility that differentiation of CAR cells into adipocytic and/or osteoblastic cells alters their niche functions. Together, our findings provide a basis for understanding

how microenvironmental niches regulate HSC maintenance and lympho-hematopoiesis within bone marrow.

EXPERIMENTAL PROCEDURES

Mice

CXCL12-GFP mice (Ara et al., 2003) and CXCL12-DTR-GFP mice were maintained on a C57BL/6 background. 5-FU (Kyowa Hakko Kirin) was injected intraperitoneally into 12- to 15-week-old mice. Imatinib (Glivec; Novartis) was applied by oral gavage (twice a day, 200 mg/kg/day). All experiments were performed under guidelines of the animal ethics committee of Institute for Frontier Medical Sciences, Kyoto University.

Generation of CXCL12-DTR-GFP Mice

The targeting vector was generated as shown in Figure 1A. The neo cassette was removed from the recombinant allele by Cre-recombinase in vivo. CXCL12-DTR-GFP mice were backcrossed to C57BL/6 mice six times. DT (MBL) was injected intraperitoneally into 12- to 15-week-old mice.

Antibodies

The antibodies used were described in Supplemental Experimental Procedures.

Flow-Cytometric Analysis and Cell Sorting

Cell-cycle analysis was performed as described in our previous publication (Sugiyama et al., 2006). For the apoptosis assay, Annexin V-FITC Apoptosis Detection Kit I (BD Biosystems) was used according to the manufacturer's instruction. All flow-cytometric experiments and cell sorting were performed using a BD FACSAria (BD Biosystems). For sorting the nonhematopoietic cell populations, cells in bone marrow fraction were obtained from femurs and tibiae by flushing and collagenase (Sigma) digestion, and cells in bone fraction were obtained from marrow-depleted bones by mechanical disruption and collagenase digestion (Mayack and Wagers, 2008).

Competitive Repopulation Assay

Unfractionated 1/20 of bone marrow cells from two femurs and tibiae (C57BL/6-Ly5.2$^+$ background) to be tested were mixed with 1×10^6 bone marrow cells of C57BL/6-Ly5.1$^+$ mice as competitor cells and were transplanted into lethally irradiated (9 Gy) C57BL/6-Ly5.1$^+$ mice. Peripheral blood cells of the recipient mice were taken 12 weeks after transplantation, and myeloid cells were analyzed by flow cytometer because their high turnover provides a good measure of HSC activity. Repopulating Units (RU) were calculated using Harrison's formula as described previously (Harrison et al., 1993).

Cell Culture and Analysis

For stromal cell-free culture, cells were sorted from wild-type mice and cultured in RPMI-1640 medium (Invitrogen) or S clone SF-3 medium (Sanko Junyaku) containing 10% fetal calf serum (FCS) with or without 20 ng/ml SCF (R&D Systems) or 1 μg/ml CXCL12. Cultured PI$^-$ viable cells were resorted and analyzed.

For adipogenic differentiation, bone marrow cell suspensions were cultured on a collagen-coated dish in DMEM supplemented with pioglitazone (Takeda Pharmaceutical) (10 μM), 10% FCS, and 5×10^{-5} M 2-β-mercaptoethanol for 7 days. To visualize lipid droplets, PFA fixation and Nile Red staining were performed. For osteogenic differentiation, bone marrow cell suspensions were cultured in α-MEM supplemented with BMP-2 (R&D Systems) (300 ng/ml), 10% FCS, and 5×10^{-5} M 2-β-mercaptoethanol for 4 days. Osteoblastic phenotypes were evaluated by the activity of ALP using Fast Red staining.

Immunohistochemical Analysis

Bone marrow sections were analyzed by immunofluorescence as described previously (Sugiyama et al., 2006). To visualize lipid droplets, Nile Red staining was performed. Confocal microscopy was performed with a LSM 510 META (Carl Zeiss).

QRT-PCR Analysis

Total RNA was isolated from sorted cells using Isogen (Nippon Gene) and treated with DNase I (Invitrogen). cDNA was synthesized using SuperScript VILO (Invitrogen) following the manufacturer's instructions. QRT-PCR analysis was performed with a Step One Plus (Applied Biosystems) using Power SYBR Green PCR Master Mix (Applied Biosystems). Values for each gene were normalized to the relative quantity of *Gapdh* mRNA in each sample. The primers used for PCR are listed in Supplemental Experimental Procedures.

Single-Cell RT-PCR Analysis

Single cells were sorted into reverse transcription buffer containing 1 U/μl RNase Inhibitor (Toyobo) and 0.4% Nonidet P-40 (Nacalai Tesque) using flow cytometry. Cell lysates were reverse-transcribed using M-MLV reverse transcriptase (Toyobo) and gene-specific reverse primers. PCR was performed by the addition of premixed hot-start PCR enzymes and buffers (AmpliTaq Gold; Applied Biosystems) containing the gene-specific forward and reverse primers designed to span introns to exclude genomic products. PCR was carried out in one round with 50 amplification cycles. The primers used for PCR are listed in Supplemental Experimental Procedures.

ELISA

Femurs were flushed with 0.3 ml of PBS containing a protease inhibitor cocktail (Sigma) and Nonidet P40 (1%). Cells were lysed by freeze and thaw, and the cell debris was removed by centrifugation and discarded. The concentrations of SCF and CXCL12 were measured using DuoSet ELISA Development kits (R&D Systems) according to the manufacturer's instructions.

Statistical Analysis

The significance of the difference between groups in the experiments was evaluated by analysis of variance followed by a two-tailed Student's t test.

SUPPLEMENTAL INFORMATION

Supplemental Information includes seven figures and Supplemental Experimental Procedures and can be found with this article online at doi:10.1016/j.immuni.2010.08.017.

ACKNOWLEDGMENTS

We thank T. Egawa, K. Tokoyoda, M. Noda, R. Kamimura, T. Ishii, and S. Uemoto for technical assistance. This work was supported by grants from the Ministry of Education, Science, Sports and Culture of Japan. Y. O., T. S., and T. N. designed and performed the experiments, analyzed the data, and prepared the paper; T. N. supervised the study; H.K. performed the experiments; G. K., N.F., and K. K. contributed materials and tools.

Received: February 3, 2010
Revised: June 12, 2010
Accepted: August 13, 2010
Published online: September 16, 2010

REFERENCES

Adolfsson, J., Borge, O.J., Bryder, D., Theilgaard-Mönch, K., Astrand-Grundström, I., Sitnicka, E., Sasaki, Y., and Jacobsen, S.E. (2001). Upregulation of Flt3 expression within the bone marrow Lin(-)Sca1(+)c-kit(+) stem cell compartment is accompanied by loss of self-renewal capacity. Immunity *15*, 659–669.

Akashi, K., Traver, D., Miyamoto, T., and Weissman, I.L. (2000). A clonogenic common myeloid progenitor that gives rise to all myeloid lineages. Nature *404*, 193–197.

Ara, T., Tokoyoda, K., Sugiyama, T., Egawa, T., Kawabata, K., and Nagasawa, T. (2003). Long-term hematopoietic stem cells require stromal cell-derived factor-1 for colonizing bone marrow during ontogeny. Immunity *19*, 257–267.

Arai, F., Hirao, A., Ohmura, M., Sato, H., Matsuoka, S., Takubo, K., Ito, K., Koh, G.Y., and Suda, T. (2004). Tie2/angiopoietin-1 signaling regulates hematopoietic stem cell quiescence in the bone marrow niche. Cell *118*, 149–161.

Arinobu, Y., Mizuno, S., Chong, Y., Shigematsu, H., Iino, T., Iwasaki, H., Graf, T., Mayfield, R., Chan, S., Kastner, P., and Akashi, K. (2007). Reciprocal activation of GATA-1 and PU.1 marks initial specification of hematopoietic stem

cells into myeloerythroid and myelolymphoid lineages. Cell Stem Cell *1*, 416–427.

Barak, Y., Nelson, M.C., Ong, E.S., Jones, Y.Z., Ruiz-Lozano, P., Chien, K.R., Koder, A., and Evans, R.M. (1999). PPAR gamma is required for placental, cardiac, and adipose tissue development. Mol. Cell *4*, 585–595.

Bianco, P., Costantini, M., Dearden, L.C., and Bonucci, E. (1988). Alkaline phosphatase positive precursors of adipocytes in the human bone marrow. Br. J. Haematol. *68*, 401–403.

Calvi, L.M., Adams, G.B., Weibrecht, K.W., Weber, J.M., Olson, D.P., Knight, M.C., Martin, R.P., Schipani, E., Divieti, P., Bringhurst, F.R., et al. (2003). Osteoblastic cells regulate the haematopoietic stem cell niche. Nature *425*, 841–846.

Cheshier, S.H., Morrison, S.J., Liao, X., and Weissman, I.L. (1999). In vivo proliferation and cell cycle kinetics of long-term self-renewing hematopoietic stem cells. Proc. Natl. Acad. Sci. USA *96*, 3120–3125.

DeKoter, R.P., and Singh, H. (2000). Regulation of B lymphocyte and macrophage development by graded expression of PU.1. Science *288*, 1439–1441.

Ficara, F., Murphy, M.J., Lin, M., and Cleary, M.L. (2008). Pbx1 regulates self-renewal of long-term hematopoietic stem cells by maintaining their quiescence. Cell Stem Cell *2*, 484–496.

Fleming, H.E., Janzen, V., Lo Celso, C., Guo, J., Leahy, K.M., Kronenberg, H.M., and Scadden, D.T. (2008). Wnt signaling in the niche enforces hematopoietic stem cell quiescence and is necessary to preserve self-renewal in vivo. Cell Stem Cell *2*, 274–283.

Foudi, A., Hochedlinger, K., Van Buren, D., Schindler, J.W., Jaenisch, R., Carey, V., and Hock, H. (2009). Analysis of histone 2B-GFP retention reveals slowly cycling hematopoietic stem cells. Nat. Biotechnol. *27*, 84–90.

Goyama, S., Yamamoto, G., Shimabe, M., Sato, T., Ichikawa, M., Ogawa, S., Chiba, S., and Kurokawa, M. (2008). Evi-1 is a critical regulator for hematopoietic stem cells and transformed leukemic cells. Cell Stem Cell *3*, 207–220.

Harrison, D.E., Jordan, C.T., Zhong, R.K., and Astle, C.M. (1993). Primitive hemopoietic stem cells: direct assay of most productive populations by competitive repopulation with simple binomial, correlation and covariance calculations. Exp. Hematol. *21*, 206–219.

Iritani, B.M., Delrow, J., Grandori, C., Gomez, I., Klacking, M., Carlos, L.S., and Eisenman, R.N. (2002). Modulation of T-lymphocyte development, growth and cell size by the Myc antagonist and transcriptional repressor Mad1. EMBO J. *21*, 4820–4830.

Kalaszczynska, I., Geng, Y., Iino, T., Mizuno, S., Choi, Y., Kondratiuk, I., Silver, D.P., Wolgemuth, D.J., Akashi, K., and Sicinski, P. (2009). Cyclin A is redundant in fibroblasts but essential in hematopoietic and embryonic stem cells. Cell *138*, 352–365.

Karsunky, H., Inlay, M.A., Serwold, T., Bhattacharya, D., and Weissman, I.L. (2008). Flk2+ common lymphoid progenitors possess equivalent differentiation potential for the B and T lineages. Blood *111*, 5562–5570.

Kiel, M.J., Yilmaz, O.H., Iwashita, T., Yilmaz, O.H., Terhorst, C., and Morrison, S.J. (2005). SLAM family receptors distinguish hematopoietic stem and progenitor cells and reveal endothelial niches for stem cells. Cell *121*, 1109–1121.

Kiel, M.J., Radice, G.L., and Morrison, S.J. (2007). Lack of evidence that hematopoietic stem cells depend on N-cadherin-mediated adhesion to osteoblasts for their maintenance. Cell Stem Cell *1*, 204–217.

Kohara, H., Omatsu, Y., Sugiyama, T., Noda, M., Fujii, N., and Nagasawa, T. (2007). Development of plasmacytoid dendritic cells in bone marrow stromal cell niches requires CXCL12-CXCR4 chemokine signaling. Blood *110*, 4153–4160.

Komori, T., Yagi, H., Nomura, S., Yamaguchi, A., Sasaki, K., Deguchi, K., Shimizu, Y., Bronson, R.T., Gao, Y.H., Inada, M., et al. (1997). Targeted disruption of Cbfa1 results in a complete lack of bone formation owing to maturational arrest of osteoblasts. Cell *89*, 755–764.

Kozar, K., Ciemerych, M.A., Rebel, V.I., Shigematsu, H., Zagozdzon, A., Sicinska, E., Geng, Y., Yu, Q., Bhattacharya, S., Bronson, R.T., et al. (2004). Mouse development and cell proliferation in the absence of D-cyclins. Cell *118*, 477–491.

Lok, S., Kaushansky, K., Holly, R.D., Kuijper, J.L., Lofton-Day, C.E., Oort, P.J., Grant, F.J., Heipel, M.D., Burkhead, S.K., Kramer, J.M., et al. (1994). Cloning and expression of murine thrombopoietin cDNA and stimulation of platelet production in vivo. Nature *369*, 565–568.

Martin, F.H., Suggs, S.V., Langley, K.E., Lu, H.S., Ting, J., Okino, K.H., Morris, C.F., McNiece, I.K., Jacobsen, F.W., Mendiaz, E.A., et al. (1990). Primary structure and functional expression of rat and human stem cell factor DNAs. Cell *63*, 203–211.

Martinez-Botas, J., Anderson, J.B., Tessier, D., Lapillonne, A., Chang, B.H., Quast, M.J., Gorenstein, D., Chen, K.H., and Chan, L. (2000). Absence of perilipin results in leanness and reverses obesity in Lepr(db/db) mice. Nat. Genet. *26*, 474–479.

Mayack, S.R., and Wagers, A.J. (2008). Osteolineage niche cells initiate hematopoietic stem cell mobilization. Blood *112*, 519–531.

Miller, C.L., Rebel, V.I., Lemieux, M.E., Helgason, C.D., Lansdorp, P.M., and Eaves, C.J. (1996). Studies of W mutant mice provide evidence for alternate mechanisms capable of activating hematopoietic stem cells. Exp. Hematol. *24*, 185–194.

Morrison, S.J., and Spradling, A.C. (2008). Stem cells and niches: mechanisms that promote stem cell maintenance throughout life. Cell *132*, 598–611.

Nagasawa, T. (2006). Microenvironmental niches in the bone marrow required for B-cell development. Nat. Rev. Immunol. *6*, 107–116.

Nagasawa, T. (2008). New niches for B cells. Nat. Immunol. *9*, 345–346.

Nagasawa, T., Kikutani, H., and Kishimoto, T. (1994). Molecular cloning and structure of a pre-B-cell growth-stimulating factor. Proc. Natl. Acad. Sci. USA *91*, 2305–2309.

Nagasawa, T., Hirota, S., Tachibana, K., Takakura, N., Nishikawa, S., Kitamura, Y., Yoshida, N., Kikutani, H., and Kishimoto, T. (1996). Defects of B-cell lymphopoiesis and bone-marrow myelopoiesis in mice lacking the CXC chemokine PBSF/SDF-1. Nature *382*, 635–638.

Nakashima, K., Zhou, X., Kunkel, G., Zhang, Z., Deng, J.M., Behringer, R.R., and de Crombrugghe, B. (2002). The novel zinc finger-containing transcription factor osterix is required for osteoblast differentiation and bone formation. Cell *108*, 17–29.

Orford, K.W., and Scadden, D.T. (2008). Deconstructing stem cell self-renewal: genetic insights into cell-cycle regulation. Nat. Rev. Genet. *9*, 115–128.

Rouleau, M.F., Mitchell, J., and Goltzman, D. (1990). Characterization of the major parathyroid hormone target cell in the endosteal metaphysis of rat long bones. J. Bone Miner. Res. *5*, 1043–1053.

Saito, M., Iwawaki, T., Taya, C., Yonekawa, H., Noda, M., Inui, Y., Mekada, E., Kimata, Y., Tsuru, A., and Kohno, K. (2001). Diphtheria toxin receptor-mediated conditional and targeted cell ablation in transgenic mice. Nat. Biotechnol. *19*, 746–750.

Santaguida, M., Schepers, K., King, B., Sabnis, A.J., Forsberg, E.C., Attema, J.L., Braun, B.S., and Passegué, E. (2009). JunB protects against myeloid malignancies by limiting hematopoietic stem cell proliferation and differentiation without affecting self-renewal. Cancer Cell *15*, 341–352.

Sugiyama, T., Kohara, H., Noda, M., and Nagasawa, T. (2006). Maintenance of the hematopoietic stem cell pool by CXCL12-CXCR4 chemokine signaling in bone marrow stromal cell niches. Immunity *25*, 977–988.

Tachibana, K., Hirota, S., Iizasa, H., Yoshida, H., Kawabata, K., Kataoka, Y., Kitamura, Y., Matsushima, K., Yoshida, N., Nishikawa, S., et al. (1998). The chemokine receptor CXCR4 is essential for vascularization of the gastrointestinal tract. Nature *393*, 591–594.

Tokoyoda, K., Egawa, T., Sugiyama, T., Choi, B.I., and Nagasawa, T. (2004). Cellular niches controlling B lymphocyte behavior within bone marrow during development. Immunity *20*, 707–718.

Visnjic, D., Kalajzic, Z., Rowe, D.W., Katavic, V., Lorenzo, J., and Aguila, H.L. (2004). Hematopoiesis is severely altered in mice with an induced osteoblast deficiency. Blood *103*, 3258–3264.

Walkley, C.R., Fero, M.L., Chien, W.M., Purton, L.E., and McArthur, G.A. (2005). Negative cell-cycle regulators cooperatively control self-renewal and differentiation of haematopoietic stem cells. Nat. Cell Biol. *7*, 172–178.

Waskow, C., Paul, S., Haller, C., Gassmann, M., and Rodewald, H.R. (2002). Viable c-Kit(W/W) mutants reveal pivotal role for c-kit in the maintenance of lymphopoiesis. Immunity *17*, 277–288.

Wilson, A., and Trumpp, A. (2006). Bone-marrow haematopoietic-stem-cell niches. Nat. Rev. Immunol. *6*, 93–106.

Wilson, A., Laurenti, E., Oser, G., van der Wath, R.C., Blanco-Bose, W., Jaworski, M., Offner, S., Dunant, C.F., Eshkind, L., Bockamp, E., et al. (2008). Hematopoietic stem cells reversibly switch from dormancy to self-renewal during homeostasis and repair. Cell *135*, 1118–1129.

Xie, T., and Spradling, A.C. (1998). decapentaplegic is essential for the maintenance and division of germline stem cells in the *Drosophila* ovary. Cell *94*, 251–260.

Yamazaki, S., Iwama, A., Takayanagi, S., Morita, Y., Eto, K., Ema, H., and Nakauchi, H. (2006). Cytokine signals modulated via lipid rafts mimic niche signals and induce hibernation in hematopoietic stem cells. EMBO J. *25*, 3515–3523.

Yamazaki, S., Iwama, A., Takayanagi, S., Eto, K., Ema, H., and Nakauchi, H. (2009). TGF-beta as a candidate bone marrow niche signal to induce hematopoietic stem cell hibernation. Blood *113*, 1250–1256.

Zhang, J., Niu, C., Ye, L., Huang, H., He, X., Tong, W.G., Ross, J., Haug, J., Johnson, T., Feng, J.Q., et al. (2003). Identification of the haematopoietic stem cell niche and control of the niche size. Nature *425*, 836–841.

Zhu, J., Garrett, R., Jung, Y., Zhang, Y., Kim, N., Wang, J., Joe, G.J., Hexner, E., Choi, Y., Taichman, R.S., and Emerson, S.G. (2007). Osteoblasts support B-lymphocyte commitment and differentiation from hematopoietic stem cells. Blood *109*, 3706–3712.

Zlotoff, D.A., Sambandam, A., Logan, T.D., Bell, J.J., Schwarz, B.A., and Bhandoola, A. (2010). CCR7 and CCR9 together recruit hematopoietic progenitors to the adult thymus. Blood *115*, 1897–1905.

Zou, Y.R., Kottmann, A.H., Kuroda, M., Taniuchi, I., and Littman, D.R. (1998). Function of the chemokine receptor CXCR4 in haematopoiesis and in cerebellar development. Nature *393*, 595–599.

Pan-histone deacetylase inhibitor panobinostat depletes CXCR4 levels and signaling and exerts synergistic antimyeloid activity in combination with CXCR4 antagonists

*Aditya Mandawat,[1,2] *Warren Fiskus,[1] Kathleen M. Buckley,[1] Kelly Robbins,[1] Rekha Rao,[1] Ramesh Balusu,[1] Jean-Marc Navenot,[3] Zi-Xuan Wang,[3] Celalettin Ustun,[1] Daniel G. Chong,[1] Peter Atadja,[4] Nobutaka Fujii,[5] Stephen C. Peiper,[3] and Kapil Bhalla[1]

[1]Medical College of Georgia Cancer Center, Augusta, GA; [2]Case Western Reserve University School of Medicine, Cleveland, OH; [3]Department of Pathology, Jefferson Medical College, Philadelphia, PA; [4]Novartis Pharmaceuticals, Cambridge, MA; and [5]Graduate School of Pharmaceutical Sciences, Kyoto University, Kyoto, Japan

Stromal cell derived factor-1 (SDF-1 or CXCL12) and its receptor CXCR4 are involved in the directional homing to the bone marrow niches and in peripheral mobilization of normal and transformed hematopoietic stem and myeloid progenitor cells. Elevated CXCR4 expression confers poor prognosis, whereas inhibition of CXCR4 signaling overcomes stroma-mediated chemoresistance in acute myeloid leukemia (AML). Here, we demonstrate that treatment with the pan-histone deacetylase inhibitor panobinostat (PS) depleted the mRNA and protein levels of CXCR4 in the cultured and primary AML cells. PS-induced acetylation of the heat shock protein (hsp) 90 reduced the chaperone association between CXCR4 and hsp90, directing CXCR4 to degradation by the 20S proteasome. PS treatment also depleted G protein–coupled receptor kinase 3, as well as attenuated the phosphorylation of AKT and ERK1/2 in AML cells, which was not affected by cotreatment with CXCL12. Compared with each agent alone, cotreatment with PS and CXCR4 antagonist AMD3100 or FC-131 synergistically induced apoptosis of cultured and primary AML cells. PS and FC-131 exerted more lethal effects on primary AML versus normal CD34$^+$ bone marrow progenitor cells. These findings support the rationale to test the in vivo efficacy of PS in enhancing the lethal effects of CXCR4 antagonists against AML cells. (*Blood*. 2010;116(24):5306-5315)

Introduction

Several mechanisms are involved in the interaction between the bone marrow microenvironment, consisting of extracellular matrix and the stromal cells and the normal and leukemia bone marrow stem and progenitor cells (BMPCs).[1,2] This interaction determines the survival, self-renewal, chemoresistance, as well as peripheral blood mobilization of BMPCs.[1,2] Among the molecular mechanisms, the interaction between the stroma cell–derived chemokine CXCL12 and its 7 transmembrane domain, G protein–coupled receptor CXCR4, is critical for activating signaling that determines the homing, survival, and mobilization of normal and leukemia BMPCs.[3-6] Binding of CXCL12 promotes CXCR4 to be phosphorylated, internalized, and incorporated into lipid rafts, which also incorporate PI3K, FAK, and Src kinases, thus enabling the clustering and phosphorylation of the receptor and the effector kinases necessary for downstream G protein–dependent and –independent signaling.[7-10] This leads to alteration in gene transcription and cell migration, as well as in promotion of survival and proliferation of normal and leukemia BMPCs.[5,6] Overexpression of CXCR4 on human CD34$^+$ progenitor cells increases their proliferation, migration, and NOD/SCID mouse repopulation potential.[11,12] In contrast, reduced retention of hematopoietic cells was noted in the bone marrow microenvironment in CXCR4$^{-/-}$ mice.[13] In addition, in acute myeloid leukemia (AML), high CXCR4 expression is associated with poor relapse-free and overall survival.[14,15] Treatment with the CXCR4 antagonist AMD3100 alone inhibited proliferation and induced differentiation in AML cells.[16] Clinical trials have demonstrated that treatment with AMD3100 alone or in combination with granulocyte colony-stimulating factor induces rapid peripheral blood mobilization of normal BMPCs.[17-19] In addition, in a genetically engineered mouse model of acute promyelocytic leukemia, administration of AMD3100 increased the circulating acute promyelocytic leukemia cell count, and cotreatment of AMD3100 with chemotherapy decreased tumor burden and improved overall survival compared with mice treated with chemotherapy alone.[20] A novel peptide CXCR4 antagonist was shown to strongly inhibit migratory and signaling responses to CXCL12 and overcome stroma-conferred chemoresistance to apoptosis in AML cells.[21] Targeting the leukemia microenvironment with CXCR4 inhibition was demonstrated to overcome resistance to kinase inhibitors and chemotherapy.[22,23] These reports have underscored the potential importance of CXCR4 as a therapeutic target in hematologic malignancies.[24,25] Based on this, novel CXCR4 antagonists, including the inverse agonist FC-131, have been developed and tested preclinically.[26,27]

Histone acetyltransferases and histone deacetylases (HDACs) play a central role in modifying the acetylation status of the lysine residues of histone and nonhistone proteins.[28] Treatment with pan-HDAC inhibitor, such as vorinostat or panobinostat (PS),

Submitted May 7, 2010; accepted August 20, 2010. Prepublished online as *Blood* First Edition paper, September 1, 2010; DOI 10.1182/blood-2010-05-284414.

*A.M. and W.F. contributed equally to this study and should be considered co–first authors.

The publication costs of this article were defrayed in part by page charge payment. Therefore, and solely to indicate this fact, this article is hereby marked "advertisement" in accordance with 18 USC section 1734.

induces hyperacetylation of histones and nonhistone proteins, including heat shock protein 90 (hsp90) in AML cells.[29-31] Hyperacetylation of hsp90 inhibits its chaperone function and promotes the proteasomal degradation of hsp90 client proteins, including FLT-3, AKT, c-RAF, and JAK2, in AML cells.[31,32] Concomitantly, HDAC inhibitor treatment has been shown to cause cell cycle growth arrest and apoptosis of AML cells.[31,32] In a phase 1 clinical trial, we observed that treatment with PS reduced AML blast cell numbers in the blood of 7 of 11 patients.[33] A recent study also showed that treatment with HDAC inhibitor lowers CXCR4 expression in human vascular endothelial cells.[34] Taken together, these findings prompted us to determine the in vitro effects of clinically relevant levels of PS on surface expression of CXCR4 and its intracellular signaling in AML cells. Our findings demonstrate that CXCR4 is chaperoned by hsp90, and treatment with PS induces hyperacetylation and inhibition of chaperone association of hsp90 with CXCR4, resulting in depletion of CXCR4 levels and downstream signaling. We further demonstrate that cotreatment with PS significantly increased the anti-AML activity of anti-CXCR4 antagonists AMD3100 and FC-131 or anti-CXCR4 antibody MAB-172.

Methods

Reagents

PS and AUY922 were kindly provided by Novartis Pharmaceuticals AG. FC-131 was obtained from the School of Pharmaceutical Sciences, Kyoto University (Kyoto, Japan). SDF-1α (CXCL12) was purchased from PeproTech. Anti-CXCR4 antibody was purchased from Abcam (ab2074). Anti–G protein–coupled receptor kinase-3 (GRK3) was obtained from Millipore. Monoclonal anti-c-Myc 9E10 was obtained from Santa Cruz Biotechnology. Anti-pFAK (Tyr397) and anti-FAK were obtained from Cell Signaling. Anti-hsp90, anti-hsp70, anti–p-AKT (Ser473), anti-AKT, anti-p-ERK1/2, anti-ERK1/2, anti–c-Raf, and anti–β-actin were obtained as previously described.[31,32] Polyclonal anti–hypoxia inducible factor-1α (HIF-1α) was obtained from Novus Biologicals. Affinity-purified polyclonal antibody against Ac-K69-hsp90 was generated by Alpha Diagnostic based on the synthetic 12–amino acid peptide flanking K69 (acetylated and unacetylated) ETLTDPSKLDSGK.[35] CXCR4 for antibody blocking experiments (MAB-172) was obtained from R&D Systems.

Cell culture

The human AML cell line OCI-AML-3 was maintained in α-minimum essential medium with 1% penicillin/streptomycin, 1% nonessential amino acids, and 10% fetal bovine serum. HL-60 cells were obtained from ATCC and maintained in RPMI with 1% penicillin/streptomycin, 1% nonessential amino acids, and 10% fetal bovine serum. HEK-293 cells expressing myc-tagged CXCR4 were generated and cultured as previously described.[36] For stabilization of HIF-1α in cells, cobalt chloride was added to a final concentration of 100μM, before treatment with PS. Logarithmically growing cell cultures were used for all experiments described.

Primary leukemia samples

Patient samples were obtained with informed consent in accordance with the Declaration of Helsinki as part of a clinical protocol approved by the Institutional Review Board at the Medical College of Georgia. As previously described,[37] mononuclear cells were separated by Ficoll-Hypaque density-gradient centrifugation, washed, and resuspended in complete RPMI 1640. The purity of the blast population was confirmed to be ≥ 80% by morphologic evaluation of Wright-stained cytospun cell preparations. $CD34^+$ mononuclear cells were purified from banked, delinked, and de-identified patient samples using immunomagnetic beads conjugated with an anti-CD34 antibody (StemCell Technologies).[37]

RNA isolation and reverse transcription PCR

Cells were harvested and total RNA was isolated using Trizol reagent (Invitrogen). Total RNA (2 μg) was reverse transcribed using a Superscript First-Stand Synthesis kit (Invitrogen). Resulting cDNAs were used for subsequent polymerase chain reaction (PCR) analysis of CXCR4, p21, p27, and β-actin. PCR reactions were performed using the following parameters: 94°C for 5 minutes followed by 35 cycles of 94°C (1 minute), 55°C (1 minute), and 72°C (1 minute). Amplified products were separated on a 2% agarose gel and recorded with an ultraviolet transilluminator. Horizontal scanning densitometry was performed with ImageQuant Version 5.2 (GE Healthcare), and the band intensity of each PCR product was compared with that of β-actin.

Detection and analysis of hsa-miR-146 in AML cells

For detection of hsa-miR-146a in AML OCI-AML3 cells, miRNAs were isolated with a kit from Applied Biosystems. Total RNA was reverse transcribed with a stem loop primer included in the TaqMan hsa-miR-146a microRNA assay following the manufacturer's protocol (Applied Biosystems). Expression of hsa-miR-146a was detected by quantitative PCR with a TaqMan probe specific to mature hsa-miR-146a. Relative expression of hsa-miR-146a was normalized against expression of 18S RNA.

Assessment of percentage nonviable cells

Untreated and drug-treated cells were stained with trypan blue (Sigma-Aldrich). The numbers of nonviable cells were determined by counting the cells that showed trypan blue uptake in a hemocytometer and reported as a percentage of untreated control cells, as previously described.[37]

Assessment of apoptosis and synergism

Untreated or drug-treated cells were stained with annexin V and propidium iodide. The percentage of apoptotic cells was determined by flow cytometry. To analyze synergism between PS and FC-131 or AMD3100 at inducing apoptosis, cells were treated with PS (5-50nM) and FC-131 (0.4-4.0μM) or AMD3100 (2.0-10.0μM) at a constant ratio for 48 hours. The percentage of apoptotic cells was determined by flow cytometry. The combination index (CI) and the fraction affected for each drug combination were obtained using the commercially available software Calcusyn Version 2.0 (Biosoft).[32,37] CI values < 1.0 represent synergism of the 2 drugs in the combination.

Cell lysis and immunoblot analyses

After designated treatments, cells were centrifuged, washed with one time phosphate-buffered saline, resuspended in TNSEV lysis buffer (50mM Tris-HCl, pH 7.5, 2mM ethylenediaminetetraacetic acid, 150mM NaCl, 1mM sodium orthovanadate, 1% Nonidet P-40) containing 20 μg/mL aprotinin, 20 μg/mL leupeptin, 1mM phenylmethylsulfonyl fluoride, and 25mM NaF, and incubated on ice for 30 minutes. For detection of HIF-1α, cells were lysed in RIPA buffer (Sigma-Aldrich). Cell lysates were centrifuged at 17 000*g* for 15 minutes to remove the nuclear and cellular debris. A total of 100 μg of total cell lysates was used for sodium dodecyl sulfate–polyacrylamide gel electrophoresis. Western blot analyses of CXCR4, hsp90, hsp70, pERK1/2, ERK1/2, pAKT (Ser 473), AKT, pGSK3β, GRK2/3, HIF-1α, and c-Raf were performed on the total cell lysates using specific antisera or monoclonal antibodies.[32,37] The expression levels of β-actin were used as the loading control for the immunoblots. Densitometry was performed with ImageQuant Version 5.2 software (GE Healthcare).

Immunoprecipitation

Precleared cell lysates were incubated for 2 hours at 4°C with anti-CXCR4 (Rb), rat anti-hsp90, polyclonal GRK3, or anti-Myc 9E10. Protein-A or -G agarose beads, as appropriate, were added to the lysate, and the mixture was incubated overnight at 4°C. The next day, the immunoprecipitates were separated from unbound protein by centrifugation, washed 3 times in TNSEV lysis buffer, and eluted from the beads by boiling in 6 times sodium dodecyl sulfate sample buffer before immunoblot analysis.[31,35]

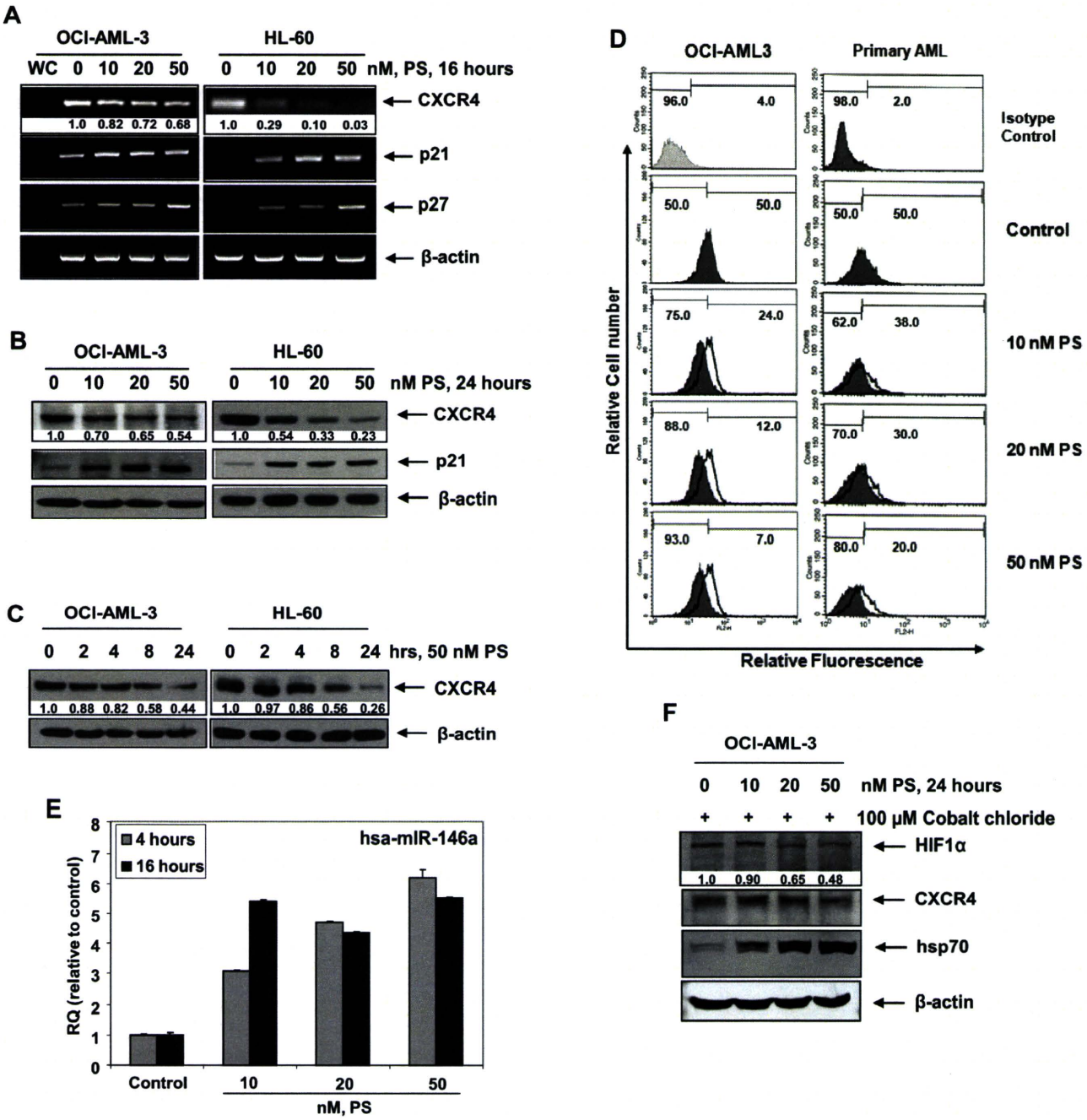

Figure 1. Treatment with PS depletes CXCR4 mRNA and protein expression in cultured and primary AML cells. (A) OCI-AML3 and HL-60 cells were treated with the indicated concentrations of PS for 16 hours. Then, total RNA was extracted and RT-PCR was performed for CXCR4, p21, and p27. A β-actin–specific PCR reaction served as a loading control for the amplification. (B) OCI-AML3 and HL-60 cells were treated with the indicated concentration of PS for 24 hours. After treatment, immunoblot analyses were performed for CXCR4 and p21 on the total cell lysates. The expression of β-actin in the lysates served as the loading control. (C) OCI-AML3 and HL-60 cells were treated with 50nM PS for the indicated times, and immunoblot analyses were performed as described in panel B. (D) OCI-AML3 and primary AML cells were treated with the indicated concentrations of PS for 24 hours. Then surface expression of CXCR4 was analyzed by flow cytometry using monoclonal phycoerythrin-conjugated 12G5 antibody. Values indicate the relative fluorescence of CXCR4 detected. (E) OCI-AML3 cells were treated with the indicated concentrations of PS for 4 and 16 hours. After treatment, total RNA was isolated and reverse transcribed with a specific stem loop primer for hsa-miR-146a. The resulting cDNAs were used for quantitative PCR with a TaqMan probe for hsa-miR-146a. Relative expression levels were normalized against 18S rRNA. (F) OCI-AML3 cells were treated with the indicated concentrations of PS for 24 hours in the presence of cobalt chloride. After treatment, cell lysates were prepared and immunoblot analyses were performed for HIF-1α, CXCR4, and hsp70. The expression levels of β-actin in the lysates served as the loading control.

AKT kinase activity assay

Cells were treated with FC-131 and/or PS for 24 hours and then stimulated with SDF-1α at 100nM for 5 minutes. Cell lysates were prepared and an AKT kinase activity kit from Cell Signaling was used according to the manufacturer's protocol. AKT kinase activity was assessed by immunoblot analysis of phosphorylated GSK3β on a recombinant GSK3β substrate. Immunoblot analyses were also performed for pAKT and total AKT.

Flow cytometry

Cell surface expression of CXCR4 was measured by flow cytometry. After an acid wash (pH 3) to elute-bound CXCL12 or FC131 from the receptor,[38] cells were incubated with a saturating concentration of phycoerythrin-conjugated anti-CXCR4 (BD Biosciences) and imaged on a FACSCalibur (BD Biosciences). phycoerythrin-conjugated anti-IgG2a served as the isotype control.

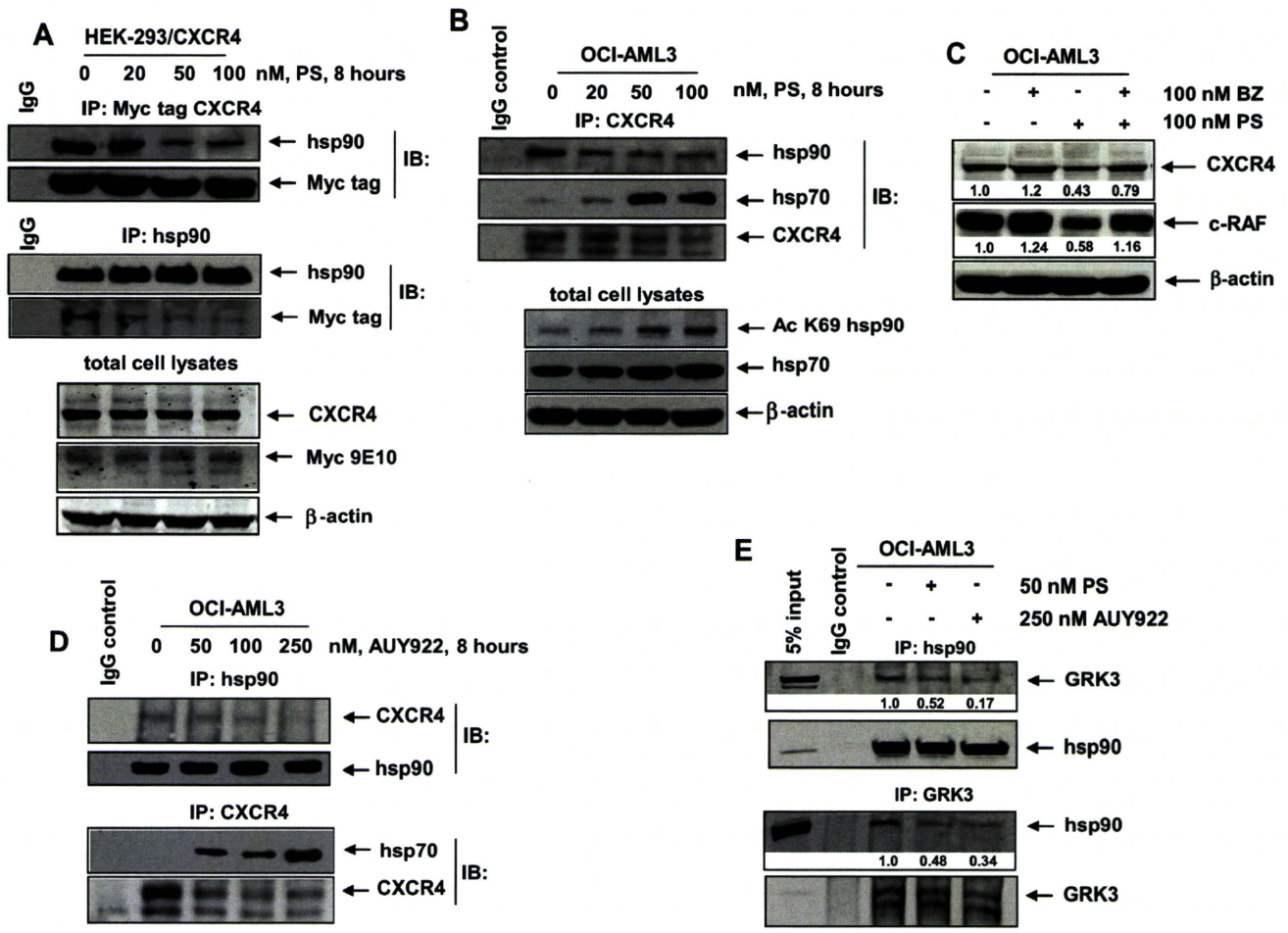

Figure 2. Treatment with PS or AUY922 depletes the binding of CXCR4 and GRK3 with hsp90 in AML cells. (A) HEK293/CXCR4 cells were treated with the indicated concentrations of PS for 8 hours. After treatment, cell lysates were prepared and Myc-tagged CXCR4 and hsp90 were immunoprecipitated. Immunoblot analyses were performed for Myc tag and hsp90 on the immunoprecipitates and total cell lysates. The expression levels of β-actin in the lysates served as the loading control. (B) OCI-AML3 cells were treated with the indicated concentrations of PS for 8 hours. At the end of treatment, cells were harvested and CXCR4 was immunoprecipitated from the total cell lysates. Immunoblot analyses were performed for CXCR4, hsp90, and hsp70 on the immunoprecipitates. Immunoblot analyses were also performed for acetylated K69 hsp90 and hsp70 in the total cell lysates. The expression levels of β-actin in the lysates served as the loading control. (C) OCI-AML3 cells were treated with the indicated concentrations of bortezomib (BZ) and PS for 8 hours. Then, total cell lysates were prepared and immunoblot analyses were performed for CXCR4 and c-RAF on the total cell lysates. The expression levels of β-actin in the lysates served as the loading control. (D) OCI-AML3 cells were treated with the indicated concentrations of AUY922 for 8 hours. At the end of treatment, cells were harvested and CXCR4 and hsp90 were immunoprecipitated from the total cell lysates. Immunoblot analyses were performed for CXCR4, hsp90, and hsp70 on the immunoprecipitates. (E) OCI-AML3 cells were treated with the indicated concentrations of PS or AUY922 for 4 hours. After treatment, hsp90 and GRK3 were immunoprecipitated from the total cell lysates. Immunoblot analyses were performed for GRK3 and hsp90 on the immunoprecipitates.

Statistics

Results are shown as mean plus or minus SE of at least 3 experiments. Data were analyzed using the paired Student *t* test. *P* values less than .05 were considered significant. All statistical sets were 2-sided.

Results

Treatment with PS attenuates the expression levels of CXCR4 mRNA and protein in cultured and primary AML cells

We first determined the effect of PS on the mRNA expression of CXCR4 in cultured AML OCI-AML3 and HL-60 cells. Treatment with PS (10-50nM) dose-dependently reduced the expression of CXCR4 mRNA while concomitantly inducing the mRNA expression of the cyclin-dependent kinase inhibitors p21 and p27 (Figure 1A). Depletion of CXCR4 mRNA was more pronounced after treatment with PS in HL-60 versus OCI-AML3 cells. Treatment with PS also depleted CXCR4 protein expression levels in a dose- and time-dependent manner, again more in HL-60 than OCI-AML3 cells (Figure 1B-C). Reduction in CXCR4 levels was noted within 4 hours with maximum depletion seen after 24 hours of treatment with PS (Figure 1C). These findings in human AML cells are consistent with the reported results demonstrating that PS treatment also reduces the mRNA and protein expression of CXCR4 in human umbilical vein endothelial cells.[34] The specificity of the antibody used here for the detection of CXCR4 was confirmed by determining that treatment with the siRNA to CXCR4 for 48 hours depleted the levels of the same 42-kDa band noted as CXCR4 in Figure 1B-C (data not shown). Next, using flow cytometry, we determined whether PS treatment also down-regulated the cell surface expression of CXCR4 in the cultured and primary AML cells. Figure 1D demonstrates that treatment with PS depleted the surface expression of CXCR4 in both OCI-AML3 and primary AML cells, as indicated by the decrease in the relative fluorescence as well as the relative decline in the percentage of positive cells in the histograms. As CXCR4 has previously been determined to be posttranscriptionally repressed by hsa-miR-146a,[39,40] we next determined the effects of PS treatment on the expression of hsa-miR146a in AML cells. As shown in

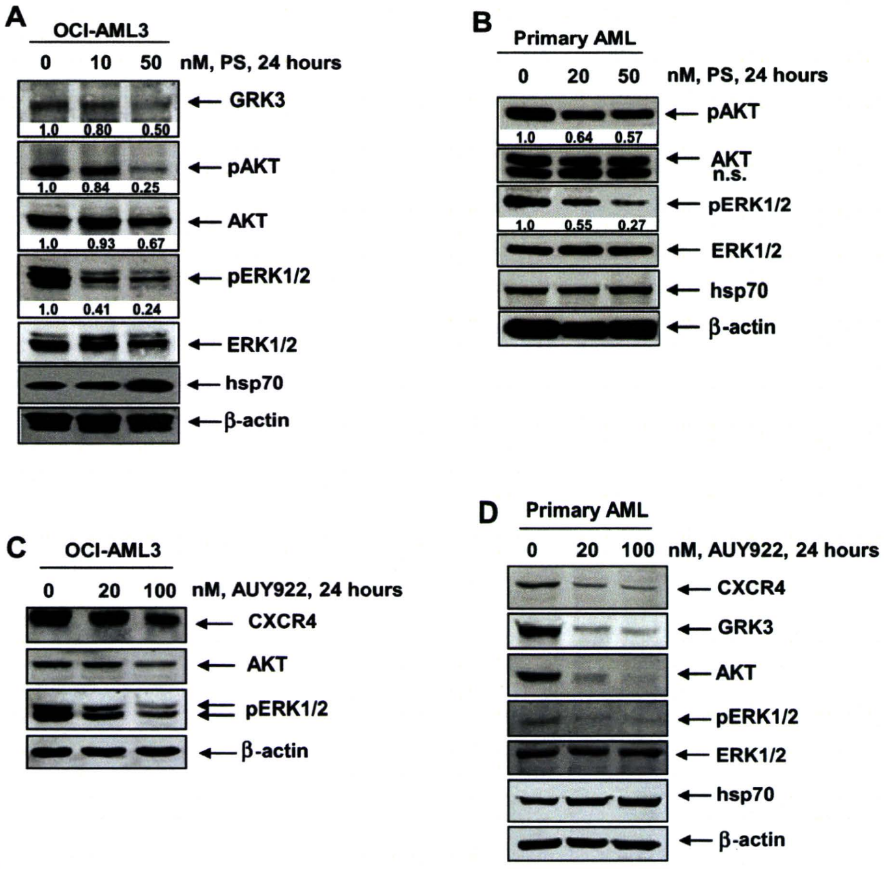

Figure 3. Treatment with PS or AUY inhibits CXCR4-mediated signaling through AKT and ERK1/2 in cultured and primary AML cells. (A) OCI-AML3 cells were treated with the indicated concentrations of PS for 24 hours. After treatment, cells were lysed and immunoblot analyses were performed for CXCR4, GRK3, pAKT (Ser 473), AKT, pERK1/2, ERK1/2, and hsp70. The expression of β-actin in the lysates served as the loading control. (B) Primary AML cells were treated with the indicated concentrations of PS for 24 hours. After treatment, cell lysates were prepared and immunoblot analyses were performed for pAKT (Ser 473), AKT, pERK1/2, ERK1/2, and hsp70. The expression of β-actin in the lysates served as the loading control. (C) OCI-AML3 cells were treated with the indicated concentrations of AUY922 for 24 hours. After treatment, cells were lysed and immunoblot analyses were performed for CXCR4, AKT, and pERK1/2. The expression of β-actin in the lysates served as the loading control. (D) Primary AML cells were treated with the indicated concentrations of AUY922 for 24 hours. After treatment, cell lysates were prepared and immunoblot analyses were performed for CXCR4, GRK3, AKT, pERK1/2, ERK1/2, and hsp70. The expression of β-actin in the lysates served as the loading control.

Figure 1E, treatment with PS causes a dose- and time-dependent induction of hsa-miR-146a up to 6-fold greater than untreated controls in OCI-AML3 cells. Because HIF-1α regulates the transcription of CXCR4 in hypoxic conditions,[41] we also determined the effects of PS treatment on the expression of HIF-1α in AML cells under chemically induced hypoxia. As Figure 1F demonstrates, treatment with PS dose-dependently depletes the expression levels of HIF-1α with concomitant down-regulation of CXCR4 expression in OCI-AML3 cells.

Treatment with PS or AUY922 induces acetylation of hsp90, inhibits the chaperone association of CXCR4 with hsp90, leading to proteasomal degradation of CXCR4

We have previously reported that, by inhibiting HDAC6, PS induces hyperacetylation of hsp90 and disruption of its chaperone function for HSF1 and other hsp90 client proteins.[31,35] This leads to the proteasomal degradation of the signaling protein kinase hsp90 client proteins (eg, c-RAF, AKT, and CDK4).[31,35] Next, we determined whether CXCR4 has chaperone association with hsp90 and whether PS treatment disrupted the binding of CXCR4 to hsp90. In HEK293 cells, with ectopic overexpression of a myc-tagged CXCR4, treatment with PS reduced the binding of myc-tagged CXCR4 and hsp90 (Figure 2A). Because the expression of the ectopic myc-tagged CXCR4 was driven by a cytomegalovirus promoter, immunoblot analysis of total cell lysates after PS treatment did not show as much decline in the levels of myc-tagged CXCR4 here as was seen in Figure 1B in the levels of the endogenous CXCR4. We confirmed that the endogenous CXCR4 also exhibited chaperone association with hsp90 in OCI-AML3 cells, which was disrupted after treatment with PS (Figure 2B). Concomitantly, PS treatment increased the levels of acetylated hsp90 as well as promoted binding of the endogenous CXCR4 to hsp70 in OCI-AML3 cells (Figure 2B). After PS treatment, reduced chaperone function of the acetylated hsp90 was also evidenced by an increase in the levels of hsp70 (Figure 2B). PS treatment–mediated reduced CXCR4 levels were partly the result of the proteasomal degradation because cotreatment with bortezomib, a proteasome inhibitor, partially restored PS-depleted CXCR4 levels (Figure 2C). A similar effect on the levels of c-RAF, a well-documented hsp90 client protein, was also noted (Figure 2C). To further confirm that CXCR4 is chaperoned by hsp90, we treated OCI-AML3 cells with the hsp90 inhibitor AUY922.[42] As demonstrated in Figure 2D, treatment with AUY922 also inhibited the binding of CXCR4 to hsp90, thereby leading to depletion of CXCR4 while inducing hsp70 levels. We also determined the effects of treatment with PS or AUY922 treatment on the chaperone association of GRK3 with hsp90. As shown in Figure 2E, treatment with PS or AUY922 for as little as 4 hours significantly inhibits the association of GRK3 and hsp90 in AML cells, consistent with GRK3 being a client protein chaperoned by hsp90.

Treatment with PS inhibits CXCR4-mediated downstream signaling molecules in cultured and primary AML cells

The GRK3 has been shown to specifically regulate CXCL12-promoted internalization and desensitization of CXCR4.[43] GRKs, including GRK2 and GRK3, are chaperoned by hsp90 and involved in phosphorylation of signaling proteins downstream of CXCR4, such as AKT and ERK1/2.[43,44] Therefore, we next determined the effects of PS treatment on the signaling proteins downstream of CXCR4 in the cultured and primary AML cells. Treatment with PS for 24 hours dose-dependently depleted the levels of GRK3,

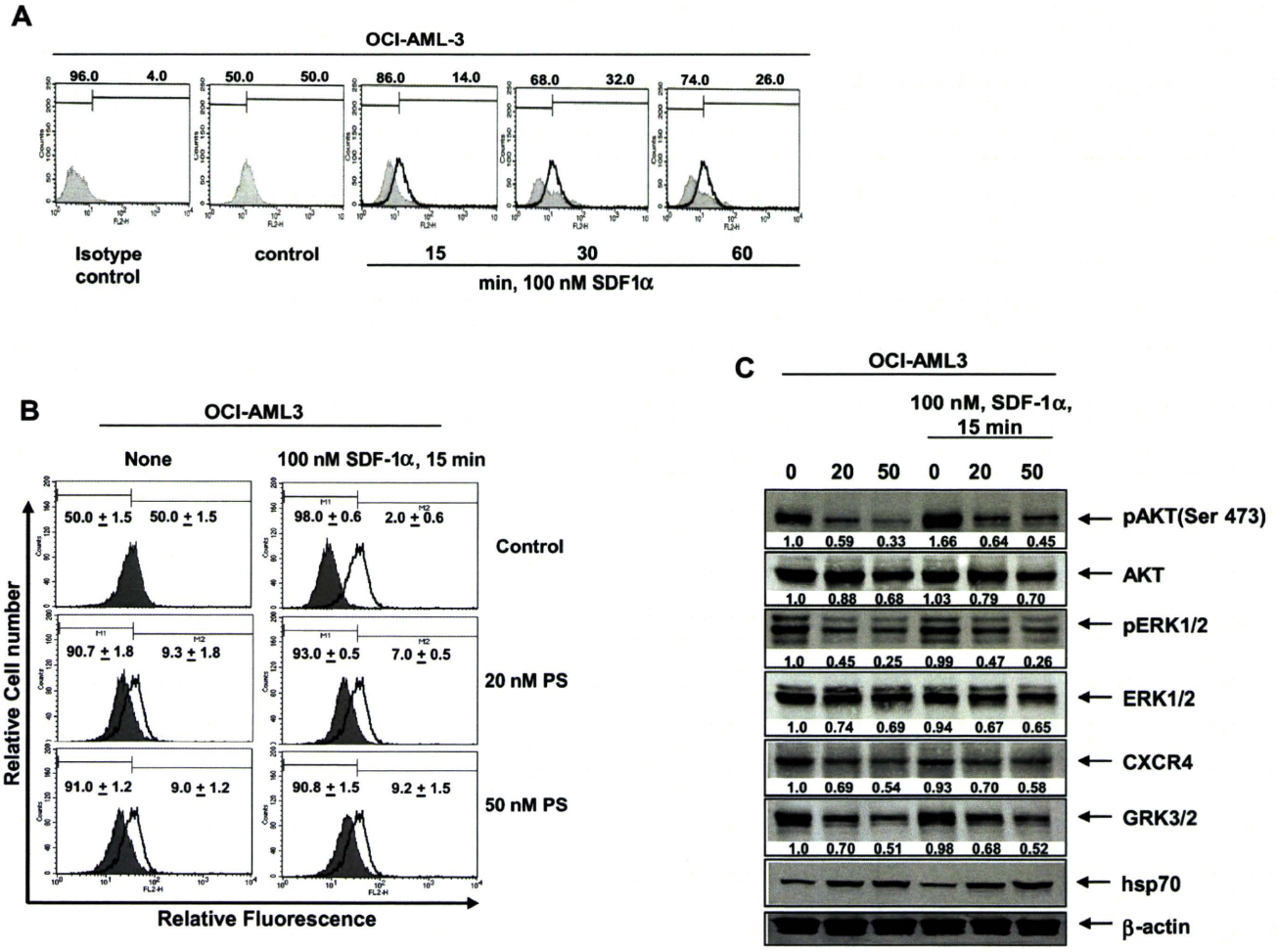

Figure 4. Cotreatment with PS inhibits SDF-1α-mediated internalization of CXCR4 in AML cells. (A) OCI-AML3 cells were treated with 100nM SDF-1α for the indicated times. After SDF-1α stimulation, cells were collected and surface expression of CXCR4 was assessed by staining the cells with anti-CXCR4 12G5 antibody and flow cytometry. (B) OCI-AML3 cells were treated with the indicated concentrations of PS for 24 hours followed by stimulation with 100nM SDF-1α for 15 minutes. Then, cells were collected and surface expression of CXCR4 was assessed by staining the cells with anti-CXCR4 (12G5) antibody and flow cytometry. (C) Immunoblot analyses of pAKT, AKT, pERK1/2, ERK1/2, CXCR4, GRK3, and hsp70 in total cell lysates from OCI-AML3 cells treated with the indicated concentrations of PS for 24 hours followed by stimulation with SDF-1α for 15 minutes. The expression of β-actin in the lysates served as the loading control.

p-AKT, AKT, and p-ERK1/2 while concomitantly inducing hsp70 expression in OCI-AML3 cells (Figure 3A). Similar effects of PS were also observed in primary AML cells (Figure 3B). Because AUY922 treatment also disrupted the chaperone association of CXCR4 with hsp90, we determined the effect of AUY922 on CXCR4 and its downstream signaling. Figure 3C demonstrates that treatment with AUY922 dose-dependently depleted the levels of CXCR4, AKT, and p-ERK1/2 while simultaneously inducing the levels of hsp70 in OCI-AML3 cells. Similar effects of AUY922 were observed on CXCR4, GRK3, AKT, and p-ERK1/2 levels in primary AML cells (Figure 3D).

Cotreatment with PS disrupts SDF-1α-mediated internalization of CXCR4 and downstream signaling

Exposure to SDF-1α (CXCL12), the ligand for CXCR4, stimulates the internalization of CXCR4, leading to the activation of downstream signaling through PI3/AKT and ERK1/2.[7] Therefore, we next determined the effects of SDF-1α alone or in combination with PS on CXCR4 levels and signaling in AML cells. As shown in Figure 4A, compared with the control cells, a short treatment (15-60 minutes) with 100nM SDF-1α alone reduced the surface expression by promoting internalization of CXCR4 levels, as detected by flow cytometry using the conformation-specific CXCR4 (12G5) antibody.[38] Treatment with PS also reduced the surface expression of CXCR4 to a similar extent as SDF-1α (Figure 4B). Cotreatment with SDF-1α and PS also showed similar reduction in the surface expression of CXCR4, although there was a slight increase with the combined treatment (Figure 4B). As has also been previously reported, exposure to SDF-1α rapidly (15 minutes) induced p-AKT levels (Figure 4C). However, pretreatment with PS reduced SDF-1α-mediated induction of p-AKT levels. In addition, PS-mediated decline in the levels of CXCR4, GRK3, AKT, p-ERK1/2, and ERK1/2 in AML cells was not affected by subsequent treatment with SDF-1α (Figure 4C). This suggests that the salutary effects of PS on disrupting CXCR4 levels and signaling are not compromised by cotreatment with SDF-1α.

Cotreatment with PS and CXCR4 antagonists or a blocking antibody for CXCR4 exerts synergistic antileukemia effects on cultured leukemic cells

We next determined the effect of PS and/or CXCR antagonists AMD3100 and FC-131 in AML cells. As has been previously reported,[32] here we also determined that treatment with PS induced

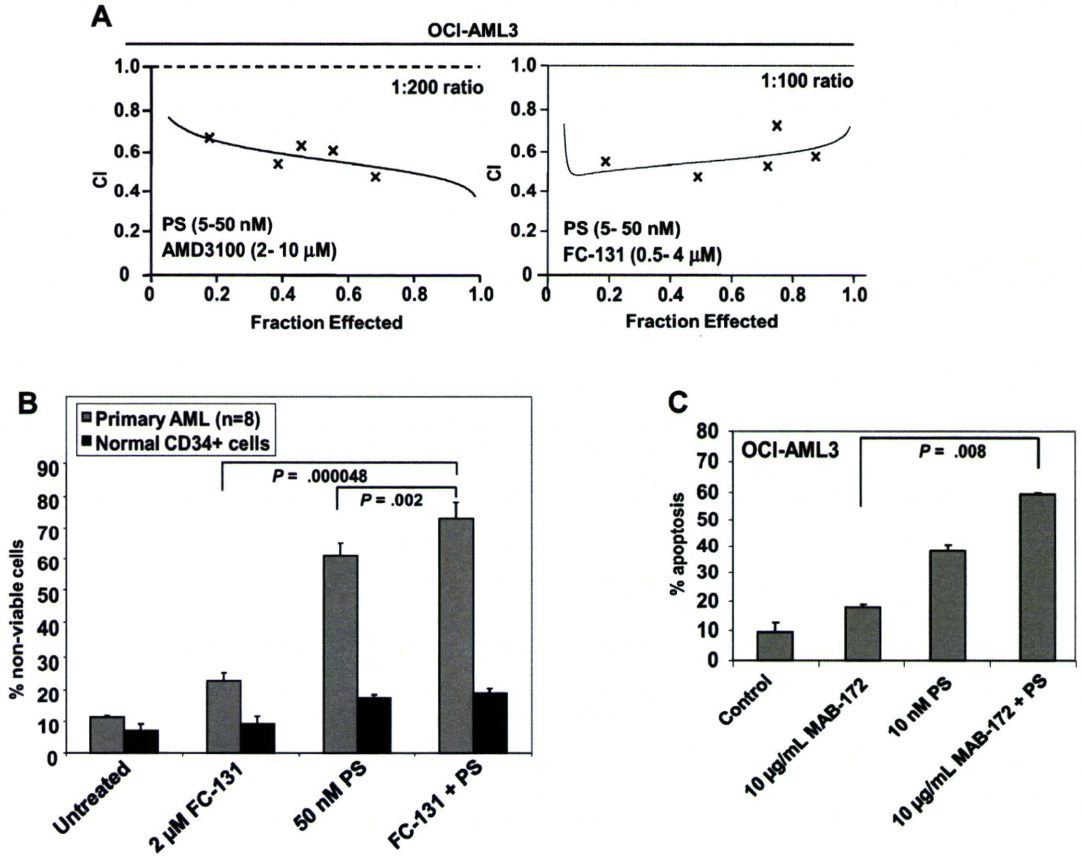

Figure 5. Treatment with AMD3100, FC-131, or a CXCR4 blocking antibody significantly increases PS-mediated lethality of AML cells. (A) Analysis of the dose-effect relationship for PS (5-50nM) and AMD3100 (2-10μM) or FC-131 (0.5-4μM) for the apoptotic effects after 48 hours of exposure in OCI-AML3 cells was performed according to the median dose effect method of Chou and Talalay. After this, the CI values were calculated using the percentage of apoptotic cells (fraction affected [FA]) by the 2 agents together. CI < 1, CI = 1, and CI > 1 represent synergism, additivity, and antagonism of the 2 agents, respectively. (B) Primary AML (n = 8) and CD34$^+$ peripheral blood mononuclear cells from healthy donors were treated with the indicated concentrations of FC-131 and/or PS for 48 hours. Then, the percentages of nonviable cells were determined by trypan blue dye uptake in a hemocytometer. (C) OCI-AML3 cells were treated with the indicated concentrations of anti-CXCR4 MAB-172 antibody and/or PS for 48 hours. Then, the percentages of apoptotic cells were determined by annexin V and propidium iodide staining and flow cytometry. Columns represent the mean of 3 experiments. Bars represent the SEM.

apoptosis of OCI-AML3 and HL-60 cells in a dose-dependent manner (data not shown). Cotreatment with AMD3100 (dose range, 2.0-10.0μM) or FC-131 (dose range, 0.5-4μM) and PS (5-50nM) induced synergistic apoptosis of OCI-AML3 cells (Figure 5A). We next compared the lethal effects of treatment with FC-131 and/or PS against primary AML cells derived from peripheral blood mononuclear cells and/or bone marrow aspirates from 8 patients with AML versus CD34$^+$ normal bone marrow progenitor cell samples from 3 normal donors. Similar to the results in the cultured cell lines, cotreatment with FC-131 significantly enhanced PS-induced cell death of primary AML cells, whereas the combination was significantly less toxic to normal CD34$^+$ cells, where it induced less than 20% cell death at 48 hours (Figure 5B). Notably, cotreatment with PS also significantly enhanced induced apoptosis of OCI-AML3 cells because of the anti-CXCR4 antibody MAB-172 (10 μg/mL; Figure 5C). We next evaluated the effect of FC-131 and PS on CXCR4 levels and signaling in AML cells. Similar to PS, treatment with FC-131 partially inhibited AKT kinase activity in OCI-AML3 cells, as measured by depletion of p-GSK3β levels (Figure 6). Cotreatment with FC-131 augmented PS-mediated depletion of AKT kinase activity represented by further decline in the levels of p-GSK3β, without affecting PS-mediated reduction in CXCR4, GRK3, p-AKT, AKT, p-ERK1/2, and ERK1/2 levels (Figure 6).

Discussion

Functional CXCR4 is expressed in AML cells and confers poor prognosis in AML.[5,6,15] CXCR4 antagonists have been shown to inhibit the survival signaling resulting from tumor microenvironment and sensitize AML cells to anti-AML therapy.[21-23] In the present studies, we demonstrate that treatment with the pan-HDAC inhibitor PS inhibits both the mRNA and protein expression of CXCR4 in cultured and primary AML cells. Although not elucidated here, it is possible that PS treatment modifies chromatin marks on the promoter of CXCR4, which enables transcriptional repression of CXCR4. Several transcriptional regulatory mechanisms have been described that regulate the expression of CXCR4.[7] These include the activity of transcriptional factors (eg, NRF1, HIF-1, NF-κB, and YY1).[7] In the present studies, we demonstrate that treatment with PS dose-dependently depletes the expression of HIF-1α, a known hsp90 client protein, in OCI-AML3 cells. Depletion of HIF-1α by PS treatment could partially explain the transcriptional down-regulation of CXCR4. Although methylation of the promoter and CXCR4 repression have been described in pancreatic cancer cells, this has not been reported in AML blasts.[45] A recent report demonstrated that megakaryopoiesis is controlled by cascade pathway where the transcription factor PLZF inhibits miR-146a, which in turn up-regulates CXCR4 expression.[40] In the

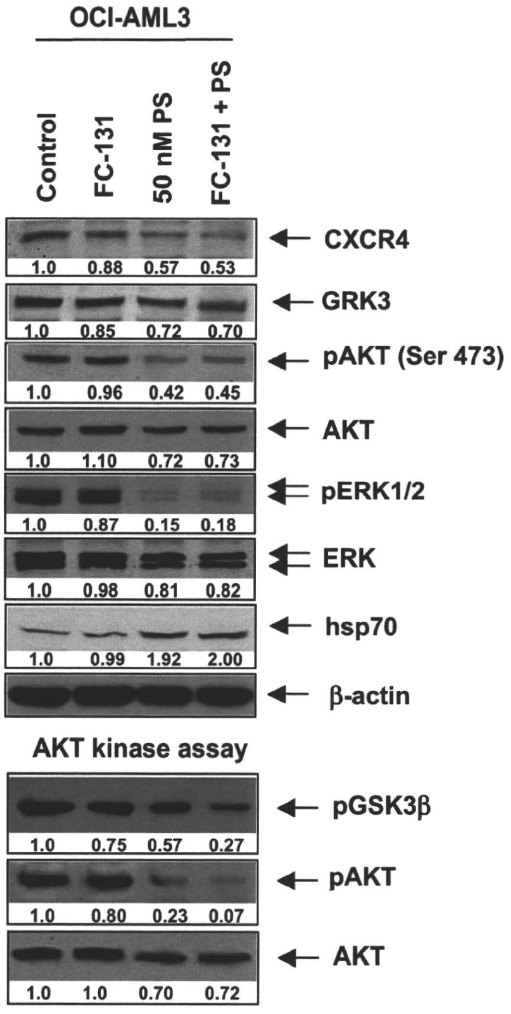

Figure 6. Treatment with FC-131 and/or PS inhibits CXCR4 signaling through AKT. OCI-AML3 cells were treated with 1 μM FC-131 and/or PS for 24 hours. Then, cells were harvested and immunoblot analyses were performed for CXCR4, GRK3, pAKT, AKT, pERK1/2, ERK1/2, and hsp70. The expression of β-actin in the lysates served as the loading control. Alternatively, activated AKT was immunoprecipitated from the total cell lysates of untreated and treated cells and used for AKT kinase activity assays. Immunoblot analyses were performed for phosphorylation of a GSK3β substrate as well as for pAKT and total AKT in the immunoprecipitates.

present studies, we demonstrate that treatment with PS dose- and time-dependently induces the levels of hsa-miR146a in AML cells. These findings indicate a second potential mechanism leading to the down-regulation of CXCR4 in AML cells.

Findings presented here demonstrate, for the first time, that CXCR4 is chaperoned by hsp90, and PS induces the acetylation and inhibits the chaperone function of hsp90, thereby promoting the proteasomal degradation and depletion of CXCR4 in AML cells. Thus, PS treatment depletes the mRNA and promotes the post-translational degradation of CXCR4 in AML cells. Chaperone association of CXCR4 with hsp90 in AML cells was further confirmed by the observation that treatment with AUY922 also disrupted the binding of CXCR4 to hsp90 and depleted CXCR4 levels. Consistent with the previous report that GRKs, including GRK3, are also chaperoned by hsp90,[43,44] findings presented here demonstrate that PS and AUY922 treatment also depletes GRK3 levels and inhibits GRK3 binding to hsp90 in AML cells. In addition, treatment with PS also lowered the levels of other signaling hsp90 client oncoproteins in AML cells, including AKT and c-RAF, which are activated by CXCL12 binding and activation of CXCR4.[7,31,32] AUY922 exerted similar activity in the cultured and primary AML cells. Activation of JAK-STAT pathway has also been reported after activation of CXCR4.[46] Treatment with PS has been shown to also down-regulate JAK-STAT signaling in human leukemia cells.[47] Taken together, these findings indicate that PS treatment is capable of attenuating multiple CXCR4-mediated signaling mechanisms that are known to confer survival advantage, as well as confer chemoresistance in AML cells.[21,22]

It has been previously reported that, on CXCL12 activation, CXCR4 is rapidly phosphorylated and internalized, activating CXCR4 signaling.[6,7] Our findings show that exposure to CXCL12 or PS also caused lowering of the surface expression of CXCR4 on AML cells. Because of its inhibitory effect on hsp90, treatment with PS also reduced the expression and activity of AKT and c-RAF independent of its effects on CXCR4. PS treatment lowered intracellular p-AKT levels and AKT kinase activity, determined against GSK3β as the AKT substrate. One possible mechanism for the down-regulation of AKT phosphorylation by HDAC or hsp90 inhibitor is that treatment with PS or AUY922 activates PP1 or another phosphatase, resulting in increased AKT dephosphorylation. Hsp90 inhibitors, such as geldanamycin, have been previously reported to increase PP1-mediated dephosphorylation of AKT in breast cancer cells.[48] Importantly, PS-mediated inhibition of the signaling kinases is not affected or compromised by the exposure of AML cells to CXCL12. This indicates that the anti-AML activity of PS mediated by its effects on CXCR4 and the signaling kinases is not abrogated by the CXCL12-CXCR4 component of the signaling for survival and chemoresistance mediated by the bone marrow microenvironment against kinase inhibitors and chemotherapy.[21-23] Other important mechanisms involved in the survival signaling of the bone marrow microenvironment niche are the VLA-4 integrins and CD44, which are expressed on AML cells that interact with stromal fibronectin and hyaluronan, respectively.[1,2,5] Because CXCR4 has been shown to cooperate with VLA-4 during AML cell adhesion and migration, lowering of CXCR4 and disrupting its signaling may also undermine the VLA-4-fibronectin–mediated survival mechanism of the bone marrow microenvironment.[5] CXCR4 antagonists, such as AMD3100 and FC-131, or anti-CXCR4 antibody, have all been shown to disrupt CXCL12-CXCR4 signaling and overcome resistance to chemotherapy and other antileukemia agents.[21-23] Here we demonstrate that cotreatment with PS significantly enhanced apoptosis of cultured AML cells induced by the anti-CXCR4 antibody MAB-172. In addition, cotreatment with PS synergistically enhanced apoptosis induced by AMD3100 and FC-131 in cultured AML cells. This was associated with greater decline in p-AKT levels and AKT kinase activity resulting from the combination, compared with treatment with each agent alone. These molecular perturbations demonstrate that combined treatment with a CXCR4 antagonist and a pan-HDAC inhibitor could attenuate AML cell homing and migration stimulated by CXCL12. In addition, importantly, the in vitro cotreatment with PS and FC-131 was significantly more lethal against primary AML cells, compared with $CD34^+$ normal BMPCs. These findings underscore the relative anti-AML selectivity of the combination of PS and a CXCR4 antagonist. Recent studies have demonstrated that a relatively longer exposure interval to the CXCR4 antagonist AMD3100 or anti-CXCR4 antibody, than those used in this study, arrested proliferation and induced features of differentiation in AML cells.[16] It is also noteworthy that treatment with pan-HDAC inhibitors has also been noted to induce differentiation in AML cells.[30] Therefore, it is possible

that, when administered in the appropriate schedule, the combined treatment with PS and CXCR4 antagonist may also induce superior differentiation of AML cells, which may contribute to the overall anti-AML activity of the combination.

Recently, the CXCR4 antagonist plerixaflor (AMD3100) was approved for hematopoietic stem cell mobilization in combination with granulocyte colony-stimulating factor for stem cell transplantation.[49] Because plerixaflor has been shown to chemosensitize AML cells after mobilization, it is now being evaluated clinically in the treatment of AML. PS is also currently in phase I/II trials in hematologic malignancies and has been demonstrated to be safe and active against AML, non-Hodgkin lymphoma, and Hodgkin disease.[50] Although not studied here in vivo, the preclinical findings that plerixaflor and PS are synergistically active against AML cells highlight the strong rationale for future studies of the combination in the therapy of AML and AML mouse models. Because the CXCR4 antagonist also exerts antitumor effects against epithelial cancers, findings presented here support the rationale for testing the combination of PS with the CXCR4 antagonist against epithelial cancers, including breast, ovarian, and lung cancers.[2,50-53]

Authorship

Contribution: A.M., W.F., K.M.B., K.R., R.R., R.B., J.-M.N., Z.-X.W., and D.G.C. performed the in vitro studies with the cultured and primary AML cells; C.U. procured and assisted in performing the studies on primary AML cells; P.A., N.F., and S.C.P. provided important reagents for the in vitro studies in cultured and primary AML cells; and K.B. planned and supervised the in vitro studies and prepared the report.

Conflict-of-interest disclosure: P.A. is an employee of Novartis Institute for Biomedical Research Inc. K.B. has received clinical and laboratory research grants from Novartis Institute for Biomedical Research Inc. The remaining authors declare no competing financial interests.

Correspondence: Kapil Bhalla, The University of Kansas Cancer Center, Kansas University Medical Center, 3901 Rainbow Blvd, 4030 Robinson, Mail Stop 1027, Kansas City, KS 66160; e-mail: kbhalla@kumc.edu.

References

1. Meads MB, Hazlehurst LA, Dalton WS. The bone marrow microenvironment as a tumor sanctuary and contributor to drug resistance. *Clin Cancer Res.* 2008;14(9):2519-2526.
2. Ayala F, Dewar R, Kieran M, Kalluri R. Contributions of bone microenvironment to leukemogenesis and leukemia progression. *Leukemia.* 2009; 23(12):2233-2241.
3. Peled A, Petit I, Kollet O, et al. Dependence of human stem cell engraftment and repopulation of NOD/SCID mice on CXCR4. *Science.*1999;283 (5403):845-848.
4. Tavor S, Petit I, Porozov S, et al. CXCR4 regulates migration and development of human acute myelogenous leukemia stem cells in transplanted NOD/SCID mice. *Cancer Res.* 2004;64(8): 2817-2824.
5. Burger JA, Burkle A. The CXCR4 chemokine receptor in acute and chronic leukaemia: a marrow homing receptor and potential therapeutic target. *Br J Haematol.* 2007;137(4):288-296.
6. Burger JA, Kipps TJ. CXCR4: a key receptor in the crosstalk between tumor cells and their microenvironment. *Blood.* 2006;107(5):1761-1767.
7. Busillo JM, Benovic JL. Regulation of CXCR4 signaling. *Biochem Biophys Acta.* 2007;1768(4): 952-963.
8. Wysoczynski M, Reca R, Ratajczak M, et al. Incorporation of CXCR4 into membrane lipid rafts primes homing-related responses of hematopoietic stem/progenitor cells to an SDF-1 gradient. *Blood.* 2005;105(1):40-48.
9. Le Y, Honczarenko M, Glodek AM, et al. CXC chemokine ligand 12-induced focal adhesion kinase activation and segregation into membrane domains is modulated by regulator of G protein signaling 1 in pro-B cells. *J Immunol.* 2005; 174(5):2582-2590.
10. Tilton B, Ho L, Oberlin E, et al. Signal transduction by CXC chemokine receptor 4: stromal cell-derived factor 1 stimulates prolonged protein kinase B and extracellular signal-regulated kinase 2 activation in T lymphocytes. *J Exp Med.* 2000; 192(3):313-324.
11. Kahn J, Byk T, Jansson-Sjostrand L, et al. Overexpression of CXCR4 on human CD34+ progenitors increases their proliferation, migration, and NOD/SCID repopulation. *Blood.* 2004;103(8): 2942-2949.
12. Burger JA, Spoo A, Dwenger A, Burger M, Behringer D. CXCR4 chemokine receptors (CD184) and alpha4beta1 integrins mediate spontaneous migration of human CD34+ progenitors and acute myeloid leukaemia cells beneath marrow stromal cells (pseudoemperipolesis). *Br J Haematol.* 2003;122:579-589.
13. Foudi A, Jarrier P, Zhang Y, et al. Reduced retention of radioprotective hematopoietic cells within the bone marrow microenvironment in CXCR4-/- chimeric mice. *Blood.* 2006;107(6):2243-2251.
14. Rombouts EJ, Pavic B, Lowenberg B, Ploemacher RE. Relation between CXCR-4 expression, Flt3 mutations, and unfavorable prognosis of adult acute myeloid leukemia. *Blood.* 2004;104(2): 550-557.
15. Spoo AC, Lubbert M, Wierda WG, Burger JA. CXCR4 is a prognostic marker in acute myelogenous leukemia. *Blood.* 2007;109(2):786-791.
16. Tavor S, Eisenbach M, Jacob-Hirsch J, et al. The CXCR4 antagonist AMD3100 impairs survival of human AML cells and induces their differentiation. *Leukemia.* 2008;22(12):2151-2158.
17. Liles WC, Broxmeyer HE, Rodger E, et al. Mobilization of hematopoietic progenitor cells in healthy volunteers by AMD3100, a CXCR4 antagonist. *Blood.* 2003;102(8):2728-2730.
18. Flomenberg N, Devine SM, Dipersio JF, et al. The use of AMD3100 plus G-CSF for autologous hematopoietic progenitor cell mobilization is superior to G-CSF alone. *Blood.* 2005;106(5):1867-1874.
19. DiPersio JF, Micallef IN, Stiff PJ, et al. Phase III prospective randomized double-blind placebo-controlled trial of plerixafor plus granulocyte colony-stimulating factor compared with placebo plus granulocyte colony-stimulating factor for autologous stem-cell mobilization and transplantation for patients with non-Hodgkin's lymphoma. *J Clin Oncol.* 2009;27(28):4767-4773.
20. Nervi B, Ramirez P, Rettig MP, et al. Chemosensitization of acute myeloid leukemia (AML) following mobilization by the CXCR4 antagonist AMD3100. *Blood.* 2009;113(24):6206-6214.
21. Zeng Z, Samudio IJ, Munsell M, et al. Inhibition of CXCR4 with the novel RCP168 peptide overcomes stroma-mediated chemoresistance in chronic and acute leukemias. *Mol Cancer Ther.* 2006;5(12):3113-3121.
22. Zeng Z, Shi YX, Samudio IJ, et al. Targeting the leukemia microenvironment by CXCR4 inhibition overcomes resistance to kinase inhibitors and chemotherapy in AML. *Blood.* 2009;113(24): 6215-6224.
23. Konopleva M, Tabe Y, Zeng Z, Andreeff M. Therapeutic targeting of microenvironmental interactions in leukemia: mechanisms and approaches. *Drug Resist Updat.* 2009;12(4):103-113.
24. Konopleva M, Andreeff M. Targeting the leukemia microenvironment. *Curr Drug Targets.* 2007;8(6): 685-701.
25. Tamamura H, Tsutsumi H, Fujii N. The chemokine receptor CXCR4 as a therapeutic target for several diseases. *Mini Rev Med Chem.* 2006;6(9): 989-999.
26. Tamamura H, Hiramatsu K, Mizumoto M, et al. Enhancement of the T140-based pharmacophores leads to the development of more potent and bio-stable CXCR4 antagonists. *Org Biomol Chem.* 2003;1(21):3663-3669.
27. Tsutsumi H, Tanaka T, Ohashi N, et al. Therapeutic potential of the chemokine receptor CXCR4 antagonists as multifunctional agents. *Biopolymers.* 2007;88(2):279-289.
28. Yang XJ, Seto E. Lysine acetylation: codified crosstalk with other posttranslational modifications. *Mol Cell.* 2008;31(4):449-461.
29. Choudhary C, Kumar C, Gnad F, et al. Lysine acetylation targets protein complexes and co-regulates major cellular functions. *Science.* 2009; 325(5942):834-840.
30. Dokmanovic M, Clarke C, Marks PA. Histone deacetylase inhibitors: overview and perspectives. *Mol Cancer Res.* 2007;5(10):981-989.
31. Bali P, Pranpat M, Bradner J, et al. Inhibition of histone deacetylase 6 acetylates and disrupts the chaperone function of heat shock protein 90: a novel basis for antileukemia activity of histone deacetylase inhibitors. *J Biol Chem.* 2005; 280(29):26729-26734.
32. George P, Bali P, Annavarapu S, et al. Combination of the histone deacetylase inhibitor LBH589 and the hsp90 inhibitor 17-AAG is highly active against human CML-BC cells and AML cells with activating mutation of FLT-3. *Blood.* 2005;105(4): 1768-1776.
33. Giles F, Fischer T, Cortes J, et al. A phase I study of intravenous LBH589, a novel cinnamic hydroxamic acid analogue histone deacetylase inhibitor, in patients with refractory hematologic malignancies. *Clin Cancer Res.* 2006;12(15):4628-4635.
34. Qian DZ, Kato Y, Shabbeer S, et al. Targeting tumor angiogenesis with histone deacetylase inhibitors: the hydroxamic acid derivative LBH589. *Clin Cancer Res.* 2006;12(2):634-642.

35. Yang Y, Rao R, Shen J, et al. Role of acetylation and extracellular location of heat shock protein 90alpha in tumor cell invasion. *Cancer Res.* 2008;68(12):4833-4842.
36. Zhang W, Navenot JM, Frilot NM, Fujii N, Peiper SC. Association of nucleophosmin negatively regulates CXCR4-mediated G protein activation and chemotaxis. *Mol Pharmacol.* 2007;72(5): 1310-1321.
37. Fiskus W, Buckley K, Rao R, et al. Panobinostat treatment depletes EZH2 and DNMT1 levels and enhances decitabine mediated de-repression of JunB and loss of survival of human acute leukemia cells. *Cancer Biol Ther.* 2009;8(10):939-950.
38. Navenot JM, Wang Z, Chopin M, Fujii N, Peiper SC. Kisspeptin-10-induced signaling of GPR54 negatively regulates chemotactic responses mediated by CXCR4: a potential mechanism for the metastasis suppressor activity of kisspeptins. *Cancer Res.* 2005;65(12):10450-10456.
39. Punj V, Matta H, Schamus S, Tamewitz A, Anyang B, Chaudhary PM. Kaposi's sarcoma-associated herpesvirus-encoded viral FLICE inhibitory protein (vFLIP) K13 suppresses CXCR4 expression by upregulating miR-146a. *Oncogene.* 2010;29: 1835-1844.
40. Labbaye C, Spinello I, Quaranta MT, et al. A three-step pathway comprising PLZF/miR-146a/CXCR4 control megakaryopoiesis. *Nat Cell Biol.* 2008;10(7):788-801.
41. Cerandini DJ, Yao D, Grogan RH, et al. Decreasing superoxide corrects defective ischemia-induced new vessel formation in diabetic mice. *J Biol Chem.* 2008;283(16):10930-10938.
42. Eccles SA, Massey A, Raynaud FI, et al. NVP-AUY922: a novel heat shock protein 90 inhibitor active against xenograft tumor growth, angiogenesis, and metastasis. *Cancer Res.* 2008;68(8): 2850-2860.
43. Luo J, Benovic JL. G protein-coupled receptor kinase interaction with Hsp90 mediates kinase maturation. *J Biol Chem.* 2003;278(51):50908-50914.
44. Salim S, Eikenburg DC. Role of 90-kDa heat shock protein (Hsp 90) and protein degradation in regulating neuronal levels of G protein-coupled receptor kinase 3. *J Pharmacol Exp Ther.* 2007; 320(3):1106-1112.
45. Sato N, Matsubayashi H, Fukushima N, Goggins M. The chemokine receptor CXCR4 is regulated by DNA methylation in pancreatic cancer. *Cancer Biol Ther.* 2005;4(1):70-76.
46. Vila-Coro AJ, Rodríguez-Frade JM, Martín De Ana A, Moreno-Ortíz MC, Martínez-A C, Mellado M. The chemokine SDF-1alpha triggers CXCR4 receptor dimerization and activates the JAK/STAT pathway. *FASEB J.* 1999;13(13):1699-1710.
47. Wang Y, Fiskus W, Chong DG, et al. Cotreatment with panobinostat and JAK2 inhibitor TG101209 attenuates JAK2V617F levels and signaling and exerts synergistic cytotoxic effects against human myeloproliferative neoplastic cells. *Blood.* 2009; 114(24):5024-5033.
48. Xu W, Yuan X, Jung YJ, et al. The heat shock protein 90 inhibitor geldanamycin and the ErbB inhibitor ZD1839 promote rapid PP1 phosphatase dependent inactivation of AKT in ErbB2 overexpressing breast cancer cells. *Cancer Res.* 2003; 63(22):7777-7784.
49. DiPersio JF, Stadtmauer EA, Nademanee A, et al. Plerixafor and G-CSF versus placebo and G-CSF to mobilize hematopoietic stem cells for autologous stem cell transplantation in patients with multiple myeloma. *Blood.* 2009;113(23):5720-5726.
50. Ottmann OG Spencer A, Prince HM, et al. Phase IA/II Study of oral panobinostat (LBH589), a novel pan-deacetylase inhibitor (DACi) demonstrating efficacy in patients with advanced hematologic malignancies [abstract]. *Blood.* 2008;112:11. Abstract 958.
51. Burger JA, Peled A. CXCR4 antagonists: targeting the microenvironment in leukemia and other cancers. *Leukemia.* 2009;23(1):43-52.
52. Huang EH, Singh B, Cristofanilli M, et al. A CXCR4 antagonist CTCE-9908 inhibits primary tumor growth and metastasis of breast cancer. *J Surg Res.* 2009;155(2):231-236.
53. Kwong J, Kulbe H, Wong D, Chakravarty P, Balkwill F. An antagonist of the chemokine receptor CXCR4 induces mitotic catastrophe in ovarian cancer cells. *Mol Cancer Ther.* 2009;8(7): 1893-1905.

Hypoxia-inducible factor-2 is a novel regulator of aberrant CXCL12 expression in multiple myeloma plasma cells

Sally K. Martin,[1] Peter Diamond,[1] Sharon A. Williams,[1] Luen Bik To,[1] Daniel J. Peet,[2] Nobutaka Fujii,[3] Stan Gronthos,[4] Adrian L. Harris,[5] and Andrew C.W. Zannettino[1]

[1]Myeloma Research Program, Division of Haematology, Centre for Cancer Biology-SA Pathology and University of Adelaide, Australia; [2]Department of Molecular Bioscience, University of Adelaide, Australia; [3]Department of Bioorganic Medicinal Chemistry, Graduate School of Pharmaceutical Sciences, Kyoto University, Japan; [4]Mesenchymal Stem Cell Group, Division of Haematology, Hanson Institute, CSCR and University of Adelaide, Australia, and [5]Weatherall Institute of Molecular Medicine, John Radcliffe Hospital, Oxford, UK

ABSTRACT

Background
Multiple myeloma is an incurable malignancy of bone marrow plasma cells. Progression of multiple myeloma is accompanied by an increase in bone marrow angiogenesis. Studies from our laboratory suggest a role for the CXCL12 chemokine in this process, with circulating levels of CXCL12 correlating with bone marrow angiogenesis in patients with multiple myeloma. While the mechanisms responsible for aberrant plasma cell expression of CXCL12 remain to be determined, studies in other systems suggest a role for hypoxia and hypoxia-inducible transcription factors.

Design and Methods
The expression of hypoxia-inducible factor protein was examined in patients' bone marrow biopsy specimens using immunohistochemistry. The hypoxic regulation of CXCL12 was examined in multiple myeloma plasma cell lines using polymerase chain reaction and western blotting. The role of hypoxia-inducible factors-1 and -2 in the regulation of CXCL12 expression was examined using over-expression and short hairpin RNA knockdown constructs, electrophoretic mobility shift assays and chromatin immunoprecipitation. The contribution of CXCL12 to hypoxia-induced angiogenesis was examined *in vivo* using a subcutaneous murine model of neovascularization.

Results
Strong hypoxia-inducible factor-2 protein expression was detected in $CD138^+$ multiple myeloma plasma cells in patients' biopsy specimens. Prolonged exposure to hypoxia strongly up-regulated CXCL12 expression in multiple myeloma plasma cells and hypoxia-inducible factor-2 was found to play a key role in this response. Promoter analyses revealed increased hypoxia-inducible factor-2 binding to the CXCL12 promoter under hypoxic conditions. Over-expression of hypoxia-inducible factor in multiple myeloma plasma cells strongly induced *in vivo* angiogenesis, and administration of a CXCL12 antagonist decreased hypoxia-inducible factor-induced angiogenesis.

Conclusions
Hypoxia-inducible factor-2 is a newly identified regulator of CXCL12 expression in multiple myeloma plasma cells and a major contributor to multiple myeloma plasma cell-induced angiogenesis. Targeting the hypoxic niche, and more specifically hypoxia-inducible factor-2, may represent a viable strategy to inhibit angiogenesis in multiple myeloma and progression of this disease.

Key words: multiple myeloma, CXCL12, hypoxia, HIF-2.

Citation: Martin SK, Diamond P, Williams SA, To LB, Peet DJ, Fujii N, Gronthos S, Harris AL, and Zannettino ACW. Hypoxia-inducible factor-2 is a novel regulator of aberrant CXCL12 expression in multiple myeloma plasma cells. Haematologica 2010; 95:776-784. doi:10.3324/haematol.2009.015628

Funding: this study was supported by grants from the National Health and Medical Research Council of Australia (ACWZ, PD, LBT, DJP, SG), the Cancer Council of South Australia (ACWZ and SG) and an Australian Postgraduate Award (SKM).

Manuscript received on August 11, 2009. Revised version arrived on September 23, 2009. Manuscript accepted on October 23, 2009.

Correspondence: Andrew Zannettino, PhD, Myeloma Research Program, Division of Haematology, Institute of Medical and Veterinary Science, PO Box 14 Rundle Mall, Adelaide 5000, Australia. E-mail: andrew.zannettino@health.sa.gov.au

The Online version of this article has a Supplementary Appendix.

Introduction

Multiple myeloma (MM) is an incurable hematologic malignancy characterized by the clonal proliferation of malignant plasma cells in the bone marrow. Accounting for approximately 1% of all cancers, MM is the second most common hematologic malignancy after non-Hodgkin's lymphoma. As for all tumors, the survival and expansion of MM plasma cells is dependent upon an adequate supply of oxygen and nutrients, and the acquisition of an angiogenic phenotype is a key event in the progression from monoclonal gammopathy of undetermined significance (MGUS) and indolent MM to active MM.[1,2]

CXCL12 is a constitutively expressed chemokine which binds primarily to the CXCR4 receptor and regulates cell growth, chemotaxis, myelopoiesis, lymphopoiesis, and development of the nervous and cardiovascular systems.[3-5] CXCL12 is highly expressed by MM plasma cells,[6] and circulating levels of CXCL12 are higher in the peripheral blood of MM patients than in age-matched normal donors and MGUS patients.[6,7] CXCL12 is an important mediator of several aspects of MM biology including transendothelial migration,[8,9] MM plasma cell migration and retention within the bone marrow,[10,11] angiogenesis,[7] and osteoclastic bone resorption.[6] Recent animal studies involving systemic injection of labeled MM plasma cells have also demonstrated that blocking the CXCL12/CXCR4 axis leads to a 20% reduction in bone marrow tumor burden.[11]

Unlike most other organs, the bone marrow microenvironment is physiologically hypoxic, a pre-requisite for normal bone marrow hematopoiesis.[12] It is well established that hypoxia is an important selective force in the evolution of tumor cells,[13] and elevated expression of the hypoxia-inducible transcription factors HIF-1 and HIF-2 has been documented in several human cancers.[14,15] HIF-1 and HIF-2 mediate adaptive responses to hypoxia by inducing the transcription of genes associated with erythropoiesis, glycolytic metabolism, cell survival and angiogenesis. While the role of hypoxia in the pathogenesis of hematologic malignancies has yet to be elucidated, recent animal studies have shown that changes in oxygen levels within the bone marrow microenvironment support the survival and expansion of MM plasma cells.[16] Furthermore, some drugs active in MM, such as bortezomib and lenalidomide, are believed to exert their effects, in part, by interfering with hypoxia-induced signaling cascades.[17,18]

HIF-1 and HIF-2 are heterodimers composed of an inducible α-subunit and a constitutively-expressed β-subunit called aryl hydrocarbon receptor nuclear translocator (ARNT). Under normoxic conditions, HIF-α subunits are functionally repressed and undergo rapid proteosomal degradation ($t_{1/2}$=5 min).[19] However under hypoxic conditions, these processes are abrogated and the stabilized HIF-α translocates to the nucleus to dimerize with ARNT. HIF-1 and HIF-2 bind to the same DNA consensus motif; however, they have overlapping but distinct target gene specificities and distinct, non-redundant physiological roles.[20,21]

In 2002, Hitchon *et al.* showed for the first time that CXCL12 expression is up-regulated by hypoxia in human synovial fibroblasts.[22] While subsequent studies extended this finding to other cell types,[23-26] the effect of hypoxia on CXCL12 expression in MM plasma cells has not been investigated. We, therefore, studied the expression of HIF-1, HIF-2 and CXCL12 in relation to hypoxia in MM and the contribution of CXCL12 to hypoxia-induced angiogenesis.

Design and Methods

Cell cultures

LP-1 cells (a human myeloma cell line) were cultured in RPMI medium supplemented with 10% fetal calf serum, 2 mM L-glutamine, 1 mM sodium pyruvate, 15 mM HEPES and 50 IU/mL penicillin-streptomycin in a humidified atmosphere at 37°C. Where specified, hypoxic culture conditions were established (less than 1% oxygen) using an anaerobic sachet (Oxoid, UK).

Immunohistochemical staining

Paraffin-embedded sections (5 μm) of MGUS (n=8) or MM (n=7) trephine specimens collected at the time of diagnosis at the Royal Adelaide Hospital were immunostained with antibodies against CXCL12 (sc-6193, Santa Cruz, CA, USA), HIF-1α (NB100-449, Novus Biologicals, CO, USA), HIF-2α (NB100-132, Novus Biologicals) and CD138 (M7228, Dako, Denmark) as previously described.[6] Studies were performed with Institutional Ethics approval following written, informed consent. Images were captured using a NanoZoomer Slide Scanner (Hamamatsu, Japan).

Stable transduction of LP-1 cells

To generate stable over-expressing cell lines, full-length cDNA encoding human CXCL12,[27] HIF-1α,[28] and HIF-2α[29] were cloned into pRUF-IRES-GFP to generate pRUF-IRES-GFP-HIF-1α, pRUF-IRES-GFP-HIF-2α and pRUF-IRES-GFP-CXCL12. Following retroviral infection of LP-1 cells, pooled cell lines were established from the top 30% of GFP-expressing cells as previously described.[27] To generate stable knock-downs, RNA duplexes targeting human HIF-1α (CCATGAGGAAATGAGAGAAATGCTT), human HIF 2α (GGGGGCTGTGTCTGAGAAGAGT) or a scrambled control (CCAAGGAGTAAGAGATAAAGGTC)[30,31] were cloned into the pFIV-H1-copGFP lentiviral vector (System Biosciences, CA, USA), and clonal cell lines generated from the top 10% of GFP-expressing cells using preparative cell sorting and single-cell deposition. For *in vivo* studies, cells were co-transduced with the SFG-NES-TGL luciferase vector[32] to enable bioluminescent detection of these cells.

Real-time polymerase chain reaction

RNA was reverse transcribed from 1 μg of total RNA using Superscript III according to the manufacturer's instructions (Invitrogen, CA, USA) and real-time polymerase chain reaction (PCR) was performed on a Rotor-Gene 3000 instrument (Corbett Life Science, Australia) using the following primers: β2-microglobulin Fwd 5'-aggctatccagcgtactcca-3' and Rev 5'-tcaatgtcggatggatgaaa-3'; human CXCL12 Fwd 5'-atgcccatgccgattcttcg-3' and Rev 5'-gtctgttgttgttcttcagcc-3'; human HIF-1α Fwd 5'-ccacctatgacctgcttggt-3' and Rev 5'-tgtcctgtggtgacttgtcc-3'; human HIF-2α Fwd 5'- ctctcctcagtttgctctgaaaa-3' and Rev 5'-gtcgcagggatgagtgaagt-3'; human vascular endothelial growth factor (VEGF) Fwd 5'- atgccaagtggtcccagg-3' and Rev 5'-cacacaggatggcttgaaga-3'; human GLUT-1 Fwd 5'- ggccaagagtgtgctaaagaa-3' and Rev 5'-cagcgttgatgccagaca-3'; human CXCR4 Fwd 5'- cagcaggtagcaaagtgacg-3' and Rev 5'-gtagatggtgggcaggaaga-3', as previously described.[27] Changes in gene expression were calculated relative to β2-microglobulin using the $2^{-\Delta Ct}$ method.[33]

Western immunoblotting

Whole cell extracts (100 μg) were separated by 8-10% sodium

dodecyl sulfate polyacrylamide gel electrophoresis (SDS-PAGE) under reducing conditions and transferred to a polyvinylidene fluoride membrane. Immunoblotting was performed using antibodies to HIF-1α (610959, BD Bioscience, CA, USA), HIF-2α (NB100-122, Novus Biologicals), and α-tubulin (ab6160, Abcam, MA, USA). Following incubation with the appropriate alkaline phosphatase-conjugated secondary antibodies, membranes were developed with ECF (GE Healthcare, UK).

CXCL12 enzyme-linked immunosorbent assay

CXCL12 protein levels in culture media were measured using a commercial immunoassay (R&D Systems, MN, USA) as previously described,[6,7] and data were normalized to the total protein content of the cells from which the supernatant was collected.

Luciferase assay

The proximal CXCL12 promoter was amplified from LP-1 genomic DNA (Fwd: 5′-gcgctcgagccatctaacggccaaagtgg-3′ and Rev: 5′-gcgaagcttggctgacggagagtgaaagtg-3′) using Pfu turbo (Stratagene, CA, USA) according to the manufacturer's instructions, and ligated into the pGL3-basic vector (E1751, Promega, WI, USA) to generate pGL3b-CXCL12. LP-1 cells (4.5×10^6) were electroporated (Bio-Rad Gene Pulser, 270V/960μF) in 500 μL in RPMI medium (supplemented with 20% fetal calf serum) with 5 μg of reporter plasmid and 10 μg of expression plasmid. Twenty-four hours after transfection, cells were cultured under normoxic or hypoxic conditions for 48 h, and their luciferase activity was assayed as previously described.[34]

Chromatin immunoprecipitation

Chromatin immunoprecipitation assays were performed using the EZ-Magna ChIP kit (Millipore, MA, USA) according to the manufacturer's instructions. Briefly, LP-1 cells (1×10^7/treatment) were cultured under normoxic or hypoxic conditions for 48 h, then cross-linked in 1% formaldehyde for 10 min at room temperature and quenched with 125 mM glycine for 5 min. Cells were washed five times in chilled phosphate-buffered saline, sonicated for 30 min (Diagenode, Belgium, 30 s pulses, 30 s rests) and immunoprecipated with magnetic beads and 5 μg primary antibody (ab199, Abcam) overnight at 4°C with rotation. The next day, complexes were eluted, sequentially washed in low salt buffer, high salt buffer, LiC buffer and TE buffer (5 min each with rotation), then eluted with 100 μg/mL proteinase K at 62°C for 2 h with rotation. Eluted DNA was purified and subjected to PCR analysis using primers directed against the HBS1 region of the CXCL12 promoter: Fwd 5′-tctaacggccaaagtggttt-3′ and Rev 5′-gccacctctctgtgtccttc-3′.

Electrophoretic mobility shift assay

The oligonucleotide for HBS1 of the CXCL12 promoter (5′-gggacagggacgtgtccccaggg-3′) was purchased from Geneworks (Australia) and the full-length product purified from non-denaturing polyacrylamide gels following established protocols.[35] Single-stranded DNA probes were prepared by end-labeling 100ng of oligonucleotide with T4 polynucleotide kinase and [γ-^{32}P] ATP (Geneworks) followed by gel purification.

Nuclear extracts were prepared from LP-1 cells following 48 h of normoxic or hypoxic culture as previously described.[36] Gel retardations were performed using 0.25 ng double-stranded ^{32}P-labeled oligonucleotide probe in a 10 μL reaction mix containing 10 mM Tris-HCl, pH 7.5, 50 mM NaCl, 1 mM $MgCl_2$, 1 mM EDTA, 5 mM DTT, 5% glycerol, 0.25 μg poly dIdC and 5 μg nuclear extract. Reaction mixes were incubated at 4°C for 30 min and resolved on 4% non-denaturing polyacrylamide gels run in 0.5x TBE buffer. For antibody blocking experiments, protein and antibody (5 μg or 10 μg) were incubated for 5 min at room temperature before adding ^{32}P-labeled probe for 20 min prior to gel loading. Gels were visualized using a Storage Phosphor Screen (GE Healthcare).

Implantation of modified LP-1 cell lines into mice

Cells (5×10^6/implant) were suspended in 200 μL chilled serum-free RPMI 1640 medium, mixed with 200 μL chilled Matrigel matrix (BD Bioscience) and subcutaneously injected into the right ventral flank of 6-week old female BALB/c nude mice. An equivalent implant containing no cells was injected into the left ventral flank. After 14 days, mice were killed humanely and Matrigel plugs were photographed and removed, and the hemoglobin content determined. Where specified, osmotic pumps (DURECT Corporation, CA, USA) containing 100 μL of the CXCR4 antagonist, T140 (4F-benzoyl-TN14003, 80 mg/mL in phosphate-buffered saline), were subcutaneously implanted in the upper dorsum 2 days prior to cell implantation.

In vivo bioluminescence imaging

Ongoing assessment of tumor growth was performed using bioluminescence imaging as previously described.[27]

Hemoglobin assessment

Excised implants were sonicated for 15 min (Diagenode, 30 s pulses, 30 s rests) in 300 μL water and centrifuged at 16,000 x g for 90 min at 4°C to remove debris. The hemoglobin content was then assessed according to instructions from Sigma (MO, USA). Briefly, homogenised tumor supernatants (50 μL/well) were added to Drabkin's solution (200 μL/well), and absorbance was read at 540 nm after 15 min. A standard curve was generated using bovine hemoglobin (Sigma).

The hemoglobin content of each cell-containing implant was initially normalized to that of the corresponding empty implant from each mouse. This value was then normalized to the bioluminescence reading obtained at the time of sacrifice, to relate the angiogenesis assessment to the number of viable cells present in the implant.

Statistical analyses

Experiments were performed in triplicate, and data are presented as mean ± standard error of measurement (SEM). Statistical analyses were performed using a one-way ANOVA with Dunnett's post-hoc test using SigmaStat® 3.0 software (Systat, IL, USA). In all cases, *P* values less than 0.05 were considered statistically significant.

Results

Expression of hypoxia-inducible factor and CXCL12 proteins in the bone marrow

Sections of bone marrow trephine specimens from patients with MGUS or MM were co-immunostained with an antibody to CD138 (a marker of MM plasma cells) and antibodies to HIF-1α, HIF-2α or CXCL12. In keeping with the findings of others,[15] weak HIF-1α expression was detected in numerous cells throughout the bone marrow (Figures 1A and 1B, panels *c* and *d*). In contrast, HIF-2α expression was restricted to CD68$^+$ macrophages (*data not shown*) and CD138$^+$ MM plasma cells (Figure 1B, panels *e* and *f*). Importantly, HIF-2α and CXCL12 proteins were both expressed in CD138$^+$ MM plasma cells (Figure 1B, panels *a*, *b*, *e* and *f*).

The hypoxic regulation of CXCL12 expression in the multiple myeloma cell line, LP-1

To examine the effect of hypoxia on CXCL12 expression in MM plasma cells, levels of *CXCL12* mRNA were measured in the MM plasma cell line, LP-1, following 6, 24 and 48 h of normoxic or hypoxic culture. Strong up-regulation of *CXCL12* mRNA was observed in response to 24 and 48 h of hypoxia (Figure 2A). This delayed hypoxic induction of CXCL12 expression was observed in three of four MM cell lines tested (U266, JIMI, and LP-1, *Online Supplementary Figure S1*), with one cell line (RPMI-8226) exhibiting no response. Using enzyme-linked immunosorbent assays, levels of CXCL12 protein were measured in LP-1 culture media following 72 h of normoxic or hypoxic culture (Figure 2B), and higher levels of CXCL12 protein were detected in hypoxic culture media (812±15.52 pg/mL) than in normoxic culture media (364±17.52 pg/mL). While hypoxic up-regulation of CXCL12 protein expression was observed in the U266 and JIMI cell lines (*data not shown*), the LP-1 cell line was selected for all the subsequent studies outlined below.

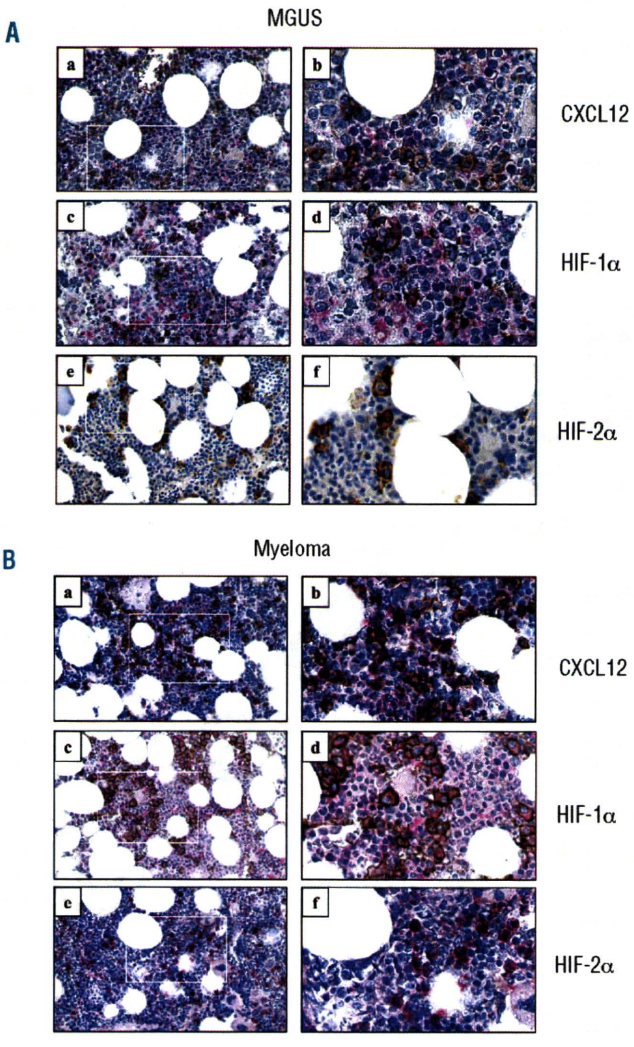

Figure 1. Expression of CXCL12, HIF-1α and HIF-2α in patients' trephine specimens. Bone marrow trephine sections from (A) MGUS and (B) MM patients at diagnosis were co-stained with CXCL12 (a and b, pink), HIF-1α (c and d, pink) or HIF-2α (e and f, pink) and CD138 (all sections, brown). Original magnifications x40 (a, c and e) and x200 (b, d and f); colors corrected after acquisition with Adobe Photoshop.

To examine the kinetics of the hypoxic induction of CXCL12 in MM plasma cells, LP-1 *CXCL12* mRNA expression was measured following 2, 4, 6, 8, 12, 24, 36, 48, 60 and 72 h of normoxic or hypoxic culture. A minimum of 24 h of continuous hypoxic exposure was required to up-regulate *CXCL12* mRNA (Figure 2C). The hypoxic induction of other HIF target genes (*GLUT1*, *CXCR4* and *VEGF*) was also examined: unlike CXCL12, their induction occurred in response to 4 - 6 h of hypoxic culture (*Online Supplementary Figure S2*). To examine the kinetics of HIF-1 and HIF-2 induction in LP-1 cells under hypoxic conditions, levels of HIF-1α and HIF-2α protein expression were measured. While HIF-1α expression was rapidly induced in response to 4-6 h of exposure to hypoxia, the induction of HIF-2α expression was delayed, requiring more than 24 h of continuous exposure to hypoxia (Figure 2C).

Over-expression and knockdown of hypoxia-inducible factors 1α and 2α in LP-1 multiple myeloma plasma cells: the effect on CXCL12

To further examine the contributions of HIF-1 and HIF-2 to the induction of MM plasma cell CXCL12 expression, LP-1 cells were engineered to stably over-express HIF-1α (LP-1-HIF-1α) or HIF-2α (LP-1-HIF-2α), and HIF over-expression confirmed by western immunoblotting (Figure 3A). Levels of *CXCL12* mRNA were then measured in LP-1-HIF-1α and LP-1-HIF-2α: it was found that *CXCL12* mRNA expression was higher in both cell lines than in the vector control (Figure 3B). Levels of CXCL12 protein were also measured in culture media collected from these transduced cell lines, and increased levels of CXCL12 protein were detected in LP-1-HIF-1α (685.0±17.05 pg/mL) and LP-1-HIF-2α culture media (805.1±20.3 pg/mL), compared to in the vector control culture media (410±28.8 pg/mL) (Figure 3C).

RNA interference (RNAi) was also used to knockdown HIF-1α or HIF-2α expression in LP-1 cells, and reduced HIF expression was confirmed by western immunoblotting (Figure 4A). Using PCR, levels of *CXCL12* mRNA were measured in these transduced cell lines, and a marked reduction in the hypoxic up-regulation of *CXCL12* was observed in response to the HIF-1α RNAi, compared to the vector and scrambled controls (Figure 4B). Strikingly, CXCL12 expression was strongly down-regulated under both normoxic and hypoxic conditions in response to the HIF-2α RNAi. CXCL12 protein levels were also measured in culture media from each of these cell lines following normoxic or hypoxic culture (Figure 4C). Importantly, the hypoxic induction of CXCL12 protein was markedly reduced in response to both the HIF-1α RNAi (653.7±53 pg/mL) and HIF-2α RNAi (520.7±43 pg/mL), compared to the vector (1079±59 pg/mL) and scrambled (936.6±21 pg/mL) controls. Considering the degree of down-regulation of CXCL12 mRNA in response to HIF-2α knockdown, the lack of a similar response at the protein level suggests that the hypoxic induction of CXCL12 involves translational and/or post-translational regulation in these cells.

Hypoxia-inducible factor-2 binds to the CXCL12 promoter under hypoxic conditions

Previous studies by Ceradini *et al.* showed that the prox-

imal CXCL12 promoter harbors two putative HIF binding sites (HBS1 and HBS2, situated at nucleotides -1,238 and -783 respectively, Figure 5A) and that the hypoxic induction of CXCL12 expression in human umbilical vein endothelial cells is mediated by the binding of HIF-1 to HBS1.[23] While the binding of HIF-1 to the CXCL12 promoter has been demonstrated previously,[23] the role of HIF-2 in the regulation of CXCL12 expression has not been examined. In this study, promoter analyses were performed to examine whether HIF-2 binds to and activates the CXCL12 promoter in MM plasma cells.

To measure changes in CXCL12 promoter activity in response to hypoxia, LP-1 cells were transiently transfected with a luciferase reporter plasmid containing the proximal CXCL12 promoter (pGL3b-CXCL12), and reporter assays performed (Figure 5B). These studies revealed that luciferase activity was increased (2-fold) under hypoxic conditions (96.8±7.2 cps) compared to normoxic conditions (53.4±10.8 cps). To delineate the role of HIF-1 and HIF-2α in the activation of the CXCL12 promoter, the pGL3b-CXCL12 construct was then transfected into the HIF-over-expressing LP-1 cell lines (Figure 5C), and increased luciferase activity was observed in LP-1-HIF-1α cells (122.4±6.3 cps) and LP-1-HIF-2α cells (211.6±36.5 cps), compared to the vector control (63.5 ±5.9 cps).

To examine the binding of HIF-2 to the CXCL12 promoter in LP-1 cells, electromobility shift assays were performed. These studies revealed strong binding of a hypoxia-inducible complex to the CXCL12 promoter (Figure 5D, *lane 2*). The presence of HIF-2 within this complex was confirmed using a HIF-2α antibody (Figure 5D, *lanes 3 and 4*). Chromatin immunoprecipitation assays were then performed to assess the level of HIF-2α binding to the CXCL12 promoter under normoxic and hypoxic conditions. Importantly, a 6-fold increase in the level of HIF-2α binding to the CXCL12 promoter was observed under hypoxic conditions (Figure 5E).

Hypoxia-inducible factor-induced CXCL12 stimulates angiogenesis in vivo

Hypoxia is a major physiological cue for triggering angiogenesis and initiates the transcription of angiogenic genes, such as those coding for VEGF,[37,38] basic fibroblast growth factor (bFGF),[39] and platelet-derived growth factor (PDGF)[40] to activate the "angiogenic switch". To examine the effect of HIF-1α and HIF-2α over-expression on MM-

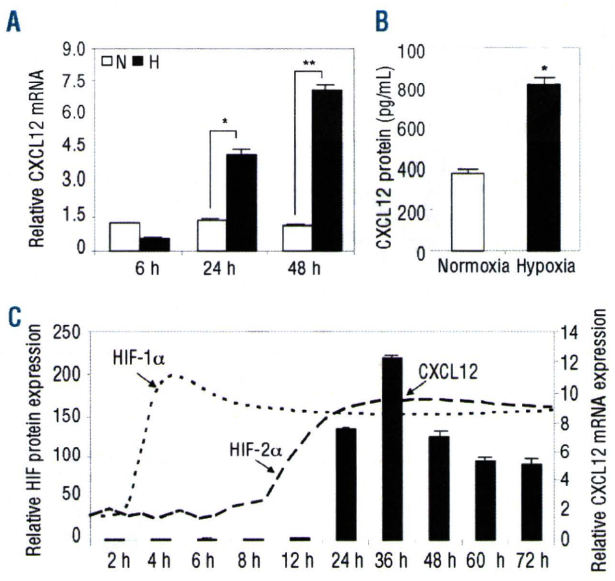

Figure 2. Hypoxic regulation of CXCL12 expression in LP-1 cells. (A) Levels of *CXCL12* mRNA expression were assessed in LP-1 cells following 6, 24 and 48 h of normoxic (white bars) or hypoxic (black bars) culture. Columns, mean (n=3); bars, SEM. *P<0.05, **P<0.001, compared to normoxia. (B) Levels of CXCL12 protein were measured in LP-1 conditioned medium following 72 h of normoxic or hypoxic culture. Columns, mean (n=3); bars, SEM. *P<0.001, compared to normoxia. (C) The hypoxic induction of *CXCL12* (black bars) mRNA, and HIF-1α (dotted line) and HIF-2α (dashed line) protein expression was examined in LP-1 cells over 72 h. Columns and dashed lines, mean (n=3); bars, SEM.

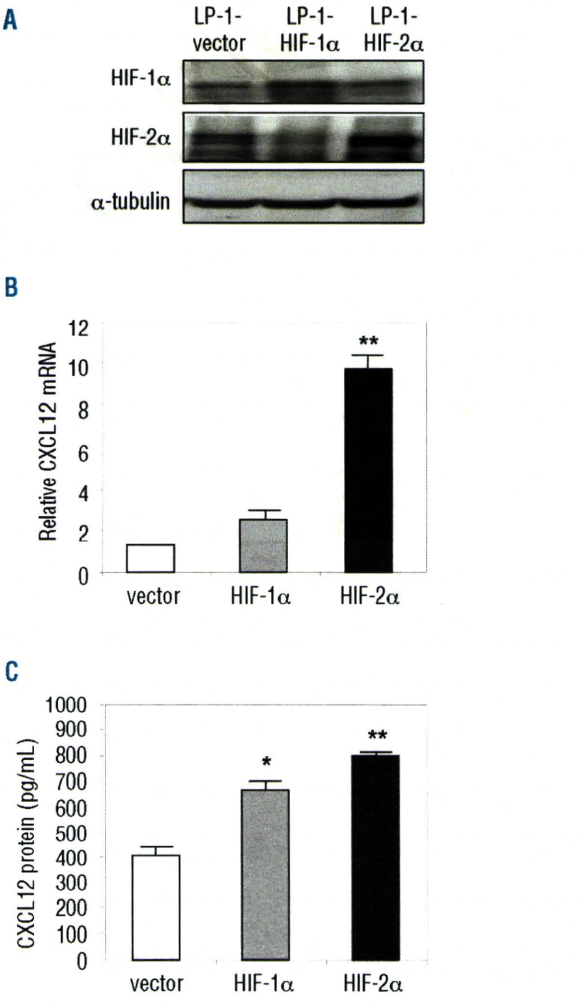

Figure 3. Stable over-expression of HIF-1α and HIF-2α in LP-1 cells. (A) LP-1 cells were engineered to stably over-express HIF-1α or HIF-2α and up-regulation of HIF protein confirmed by western immunoblotting. (B) Levels of *CXCL12* mRNA expression were examined in the HIF over-expressing LP-1 cell lines. Columns, mean (n=3); bars, SEM. **P<0.001, compared to vector control. (C) Levels of CXCL12 protein were measured in conditioned media from the HIF over-expressing cell lines. Columns, mean (n=3); bars, SEM. *P<0.05, **P<0.001, compared to vector control.